Oceanography and Marine Biology

AN ANNUAL REVIEW

Volume 42

Editors

R.N. GIBSON

R.J.A. ATKINSON

J.D.M. GORDON

Founder Editor

HAROLD BARNES

CRC PRESS

OCEANOGRAPHY
and
MARINE BIOLOGY

AN ANNUAL REVIEW

Volume 42

OCEANOGRAPHY and MARINE BIOLOGY

AN ANNUAL REVIEW

Volume 42

Editors

R.N. Gibson
Scottish Association for Marine Science
The Dunstaffnage Marine Laboratory
Oban, Argyll, Scotland
robin.gibson@sams.ac.uk

R.J.A. Atkinson
University Marine Biology Station Millport
University of London
Isle of Cumbrae, Scotland
r.j.a.atkinson@millport.gla.ac.uk

J.D.M. Gordon
Scottish Association for Marine Science
The Dunstaffnage Marine Laboratory
Oban, Argyll, Scotland
john.gordon@sams.ac.uk

Founded by Harold Barnes

CRC PRESS

Boca Raton London New York Washington, D.C.

CRC Press
Taylor & Francis Group
6000 Broken Sound Parkway NW, Suite 300
Boca Raton, FL 33487-2742

Version Date: 20130919

International Standard Book Number-13: 978-0-203-50781-0 (eBook - PDF)

Visit the Taylor & Francis Web site at
http://www.taylorandfrancis.com

and the CRC Press Web site at
http://www.crcpress.com

Contents

Preface

The 42nd volume of this series contains eight reviews written by an international array of authors that, as usual, range widely in subject and taxonomic and geographic coverage. The majority of articles were solicited, but the editors always welcome suggestions from potential authors for topics they consider could form the basis of appropriate contributions. Because an annual publication schedule necessarily places constraints on the timetable for submission, evaluation, and acceptance of manuscripts, potential contributors are advised to make contact with the editors at an early stage of preparation so that the delay between submission and publication is minimised.

The editors gratefully acknowledge the willingness and speed with which authors complied with the editors' suggestions, requests, and questions. This year has also seen further changes in publisher (CRC Press) and in the editorial team and it is a pleasure to welcome Dr. J.D.M. Gordon as a co-editor for the series.

CONVECTIVE CHIMNEYS IN THE GREENLAND SEA: A REVIEW OF RECENT OBSERVATIONS

PETER WADHAMS
Scottish Association for Marine Science, Dunstaffnage Marine Laboratory, Oban PA37 1QA, Scotland, and
Department of Applied Mathematics and Theoretical Physics, University of Cambridge, Wilberforce Road, Cambridge CB3 0WA, England
E-mail: peter.wadhams@sams.ac.uk
p.wadhams@damtp.cam.ac.uk

Abstract The nature and role of chimneys as a mode of open-ocean winter convection in the Greenland Sea are reviewed, beginning with a brief summary of Greenland Sea circulation and of observations of convection and of the resulting water structure. Then recent observations of long-lived chimneys in the Greenland Sea are described, setting them within the context of earlier observations and models. The longest-lived chimney yet seen in the world ocean was discovered in March 2001 at about 75˚N 0˚W, and subsequent observations have shown that it has survived for a further 26 months, having been remapped in summer 2001, winter 2002, summer 2002, and April–May 2003. The chimney has an anticyclonically rotating core with a uniform rotation rate of f/2 to a diameter of 9 km; it passes through an annual cycle in which it is uniform in properties from the surface to 2500 m in winter, while being capped by lower-density water in summer (primarily a 50-m-thick near-surface layer of low salinity and a 500-m-thick layer of higher salinity). The most recent cruise also discovered a second chimney some 70 km NW of the first, and accomplished a tightly gridded survey of 15,000 km^2 of the gyre centre, effectively excluding the possibility of further chimneys. The conclusion is that the 75˚/0˚chimney is not a unique feature, but that Greenland Sea chimneys are rare and are probably rarer than in 1997, when at least four rotating features were discovered by a float survey. This has important implications for ideas about chimney formation, for deepwater renewal in the Greenland Sea, and for the role of Greenland Sea convection in the North Atlantic circulation.

Convection in the world ocean

Open-ocean deep convection is a process of ventilation, not associated with coastal processes, that feeds the global thermohaline circulation. It occurs in winter at only three main Northern Hemisphere sites (Greenland, Labrador, and Mediterranean Seas) as well as in the Weddell Sea and a small number of other locations in Antarctica. These sites are of small geographical extent, occupying only a few thousandths of the area of the world ocean, yet they are of great importance for climate, because it is only through deep ventilation that a complete vertical circulation of the ocean can take place, with dissolved gases and nutrients cycling back into the depths. In some cases intense atmospheric cooling alone increases the surface water density to the point where the overturning and sinking can occur. In others, sea ice is involved. The modes of convection at the various key sites have been reviewed by Marshall & Schott (1999).

0-8493-2727-X/04/$0.00+$1.50
Oceanography and Marine Biology: An Annual Review 2004 **42**, 29–56

In the case of the Northern Hemisphere, the Greenland Sea and the Labrador Sea form the sinking component of the Atlantic thermohaline circulation, or meridional overturning circulation, and any changes in convection at these two sites will therefore have an impact on global climate, and most certainly on northwest European climate, which is so dependent on the strength of the Gulf Stream (Rahmstorf & Ganopolski 1999). Since the 1980s a series of international, mainly European, research programmes has focused on the central Greenland Sea gyre region and its structure in winter. Initially attention focused on the relatively shallow (1000–1400 m) convection that occurs over the whole central gyre region, due to either plumes or mixed-layer deepening. But from 1997 onward the observed presence of chimneys, long predicted, has changed our view of the character of mid-gyre convection. Convection in the Labrador Sea has also been studied intensively in recent years, primarily by a single large international programme (Lab Sea Group 1998).

Recently Pickart et al. (2003) showed that at times of high positive North Atlantic Oscillation (NAO), an overturning occurs in the Irminger Sea, giving a third convection site within the northern North Atlantic region. The Irminger Sea had been invoked as a possible convection site in early papers from the 1960s and 1970s, but had subsequently been disregarded. The observational evidence produced by Pickart et al. (2003) shows that convection can occur south of the Denmark Strait overflow but not necessarily in phase with convection from the Labrador Sea, giving an added complexity to the question of the relation between overall convection volume and the NAO index. In simplified terms, a positive NAO index corresponds to an anomalous low over Iceland, which induces enhanced cold northwesterly winds over the Labrador Sea (giving increased convection) and enhanced warm easterly winds over the Greenland Sea (reducing convection), a seesaw effect that is reversed when the NAO changes sign. Because the volume of Labrador Sea convection is in general greater than that of the Greenland Sea, it is expected that Northern Hemisphere convection volume will be greatest during positive NAO periods. However, modelling studies (Wood et al. 1999) suggest that due to global warming, convection in the Labrador Sea is set to diminish and may vanish altogether in 30 yr, regardless of the state of the NAO.

This review focuses on the Greenland Sea, surveys the recent observations of chimneys, from which the results are in many cases still in press, and attempts to draw some conclusions about the nature and role of Greenland Sea chimneys in the overall scheme of convection.

The geography of the Greenland Sea gyre

Convection in the Greenland Sea occurs in the centre of the Greenland Sea gyre, at about 75°N 0–5°W. This region is bounded to the west by the cold, fresh polar surface water of the southward-flowing East Greenland Current (EGC), advecting ice and water of polar origin into the system from the Arctic Basin. To the east it is bounded by the warm northward-flowing Norwegian Atlantic Current (Figure 1, in the colour insert following page 56), which changes its name farther north to the West Spitsbergen Current (WSC). Its boundary to the south is a cold current that diverts from the East Greenland Current at about 72–73°N because of bottom topography and wind stress. This is called the Jan Mayen Polar Current, and in winter, at least until recent years, it develops its own local ice cover of frazil and pancake ice due to high-ocean-atmosphere heat fluxes acting on a cold water surface, forming a tongue-shaped ice feature called Odden (Norwegian: headland), which can be up to 250,000 km^2 in area (Figure 2, see colour insert). Its curvature embraces a bay of ice-free water, called Nordbukta, which tends to correspond with the gyre centre. In heavy ice years Nordbukta becomes ice covered, so that the two features together form a bulge in the ice edge trend at these latitudes.

Frazil–pancake ice can grow very quickly, and with the initial skim having a salinity of 12–18, more than half of the brine content of the freezing sea water is rejected immediately back into the ocean. The salinity increase caused by brine rejection may be a more important trigger than surface cooling for overturning of the surface water and the formation of convective plumes that carry surface water down through the pycnocline into the intermediate and deep layers. Of course, over a whole year ice formation and ice melt balance out so that the net overall salt flux is zero. However, the ice formation and melt regions are geographically separated. The ice growth occurs on the western side of Odden, while the ice formed is moved eastward by the wind to melt at the eastern, outer edge of the ice feature. Consequently, there is a net positive salt flux in a zone that is found to be the most fertile source of deep water. The connection between Odden ice and convection has been explored in salt flux models that take account of ice formation, ice advection, and brine drainage (e.g., Wilkinson & Wadhams 2003). Evidence from recent hydrographic and tracer studies has shown that convection has become weaker and shallower in recent years, while there has also been a decline in ice formation within Odden, but it is still an open question whether there is a causal association between these two sets of changes. Also, it is not yet clear whether the decline of Odden is a trend deriving from global warming or a cyclic effect associated with a particular pattern of wind field over the Greenland Sea. Wadhams et al. (1996), Toudal (1999) and Comiso et al. (2001) have discussed the interannual variability of Odden and have shown how on increasingly frequent occasions during the last decade (1994, 1995, and 1999 onward), it has failed altogether to develop.

The eastern edge of the East Greenland Current corresponds to the position of the main Arctic ice edge in winter, giving rise to interactions that result in ice edge eddies and other phenomena, but in summer the ice retreats westward and northward. In winter of an average year the ice reaches Kap Farvel, whereas in summer the ice edge retreats to about 74°N, although there is a large interannual variability. In September 1996, for instance, there was a period of a month in which no ice occurred within Fram Strait. Figure 3 (see colour insert) shows the magnitude of the 10-yr variability (1966–75) for a winter and a summer month. It can be seen that the East Greenland Current and Barents Sea together offer the longest stretch of marginal ice zone in the Arctic, facing onto the Norwegian–Greenland Sea, which is well known for its storminess. Ice is transported into the Greenland Sea from the Arctic Ocean at a rate of some 3000 $km^3\ yr^{-1}$ and melts as it moves southward, so that the Greenland Sea as a whole, when averaged over a year, is an ice sink and thus a freshwater source. The freshwater supplied to the Greenland Sea gyre from the Arctic Ocean via the EGC has a flux that varies greatly from year to year as well as seasonally, and this variability may exert control over convection by altering the freshwater input to the surface waters of the convective region during summer (Aagaard & Carmack 1989).

The role of the Greenland Sea as the main route for water and heat exchanges between the Arctic Ocean and the rest of the world also extends to subsurface transport. It is a part of the Arctic Intermediate Water (AIW) formed during convection in the Greenland Sea that ventilates the North Atlantic (Aagaard et al. 1985) and supplies the Iceland–Scotland overflow (Mauritzen 1996a,b). Another source of AIW formation is the Norwegian Atlantic Current, which enters the Arctic Ocean (as the WSC), circulates, and enters the Greenland Sea through Fram Strait as the EGC, moving down toward Denmark Strait (Rudels et al. 1999). The Arctic circumpolar current experiences numerous branchings and mergings, in particular in Fram Strait. This has been described by a number of authors (Quadfasel et al. 1987, Foldvik et al. 1988, Gascard et al. 1995) and modelled in detail by Schlichtholz & Houssais (1999a,b).

Historically, ice conditions in the Greenland Sea were first described in the classic work of William Scoresby (1815, 1820), while the pioneering oceanographic work of Helland-Hansen & Nansen (1909) early this past century began an era of continuous effort, much of it by Scandinavian oceanographers, which has led to improved understanding of the complex water mass structure. The present era of intensive work on Greenland Sea convection began with an international research programme known as the Greenland Sea Project (GSP), which started in 1987 with an intensive field phase in 1988–89. GSP studied the rates of water mass transformation and transport, the food chain dynamics, the life cycles of dominant plankton species, and particulate export (GSP Group 1990). It was realised that insufficient attention had been paid to the carbon cycling and export in this area, with exceptions such as the long-term sediment trap programme of Honjo et al. (1987)

and two expeditions that collected inorganic carbon data in this region during the early 1980s (Brewer et al. 1986, Chen et al. 1990). New data suggested that convection may be associated with a carbon flux that is significant in the removal, or sequestration, of anthropogenic CO_2 from the atmosphere: surface waters in the region have consistently been found to be significantly undersaturated in dissolved CO_2 (Skjelvan et al. 1999, Hood et al. 1999).

In 1993 GSP evolved into the European Subpolar Ocean Programme (ESOP), an EU project coordinated by the present author, with an intensive field phase during winter 1993 and further field operations in 1994 and 1995, with a final study of the 1996 Odden development (Wadhams et al. 1999). In 1996 a successor programme began called ESOP-2, coordinated by E. Jansen, which focused on the thermohaline circulation of the Greenland Sea and which lasted until 1999. Most recently, CONVECTION (2001–3), another EU project coordinated by the present author, has concentrated on the physical processes underlying convection and has involved winter and summer cruises each year.

Observations of convection before 2001

Depth of overturning

During the period since about 1970 deep winter convection in the Greenland Sea was thought to have ceased. Evidence from the temperature–salinity (T,S) structure of Greenland Sea Deep Water (GSDW) suggested that significant renewal by surface ventilation last occurred in 1971. Tracer measurements using chlorofluoromethane suggested that convection below 2000 m stopped before 1982, while convection below 1500 m decreased from 0.8–1.2 Sv before 1982 to 0.1–0.38 Sv during 1983–89 (Rhein 1991) and less than 0.14 Sv during 1989–93 (Rhein 1996), results supported by tritium observations (Schlosser et al. 1991). Direct observations of deep convection from oceanographic surveys, and interpretations from tomography, showed that a depth of 1800 m was achieved in 1989 (Schott et al. 1993, Morawitz et al. 1996), but that in more recent years the typical depth was 1000–1200 m. Depths exceeding 2000 m were last observed in 1974, except for a single surface-to-bottom event in 1984 (Alekseev et al. 1994).

The 1997 chimney(s)

During the 1996–97 winter field season of ESOP-2, a series of subsurface floats was deployed in the central gyre region by Gascard (1999). Five of 16 floats released within the region 74–76˚N, 1˚E–4˚W, at depths between 240 and 530 m, adopted anticyclonically rotating trajectories of small radius (Figure 4, see colour insert). In most cases the centre of rotation slowly advected around the region, but in the case of a buoy positioned at 75˚N 0˚W the centre remained essentially stationary for several months. In this case, reported in detail by Gascard et al. (2002), the buoy remained for 150 days near the gyre centre, recording an ambient temperature of about –1˚C, before spiralling outward. Their interpretation of the trajectory was that the buoy was trapped in an eddy with a core of diameter about 5 km, which rotated as a solid body, and a more slowly rotating "skirt" extending out to a radius of 15 km, in which the angular velocity decreased with increasing distance from the centre. The relative vorticity of the core was about –f/2, where f is the planetary vorticity, diminishing to –f/8 at 8-km radius.

At first the apparent subsurface eddies in which the floats were trapped were not identified with chimneys, but in May 1997 a section along 75˚N included one station at 0˚W that showed a uniform temperature–salinity structure extending from near the surface to some 2200 m. The section was associated with an experiment to release SF_6 tracer within the Greenland Sea (Watson et al. 1999), and it was found that this station displayed low SF_6 levels and high levels of chlorofluorocarbons (CFCs) and dissolved oxygen.

The conclusion reached by Gascard et al. (2002) was that the station and the float trajectory were indicators of a chimney (although in their paper they continued to describe it as an eddy) at 75°N 0°W (leaving open the question of whether the other floats were trapped in other chimneys). The winter of 1996–97 had been extremely cold, with air–sea heat fluxes in January 1997 as high as 1400 W m^{-2} (average for a month about 500 wm^{-2}). Their conclusion was that during this month surface water, cooled to about –1°C, mixed with the stratified rotating water mass that comprised the gyre centre and produced rotating lenses by a mechanism described by Gill (1981). Such lenses, however, were observed in tank experiments (Hedstrom & Armi 1988) to have a fast-spin down phase that would correspond to a lifetime of about 70 rotations, about 4–6 months. Thus, the observed eddy or eddies were actually being measured throughout their lifetimes, and their apparent expulsion of the floats from the cores of the eddies may have corresponded to the core collapse. Lherminier et al. (2001) used the data of Gascard et al. and large-eddy simulation to show that isobaric floats are attracted into convergence zones naturally generated by convection, showing that floats are an efficient means of detecting those chimneys that do exist in the central gyre.

Gascard et al. (2002) carried out a binary water mass analysis and concluded that the water structure in the eddy could have been generated by a mixture of 36% Arctic surface water (presumably from the East Greenland Current) and 64% return Atlantic water, which recirculates at mid-depth (some 500 m) in the East Greenland Current. The surface temperature would have been –1.61°C and salinity 34.81, while the return Atlantic water was at –0.78°C and 34.89. No account was taken of increase of surface salinity due to sea ice formation.

Thus, the mechanism proposed by Gascard et al. (2002) calls for submesoscale eddies to be generated by geostrophic adjustment and diapycnal mixing between surface polar waters and subsurface modified Atlantic water. The mechanism by which the mixing occurs, however, was not mentioned, and thus does not necessarily involve sinking of the surface water, but possibly lateral mixing where water masses meet. Some kind of mixing allows Arctic surface water to be injected into a rotating stratified water mass (the return Atlantic water), and this produces the subsurface eddy field. The eddies are coherent and have lifetimes of a few months. Gascard et al. (2002) speculated that such an eddy could precondition water masses for convective activity in the following winter season: they could then form foci to concentrate further convection after erosion of the layer of less dense water that caps the core during the summer. Such a statement suggests a picture of an individual eddy collapsing but inducing the formation of another in the same region during the subsequent winter.

A problem of nomenclature occurs in Gascard et al. (2002). The features are described throughout as *eddies* or as *submesoscale coherent vortices*. The latter terminology has, up to now, been considered specific to a kind of long-lived coherent subsurface eddy found in the Mediterranean outflow into the Atlantic, the so-called Meddy (Armi et al. 1989). On the other hand, the term *chimney* originated as a descriptor of the first such uniform, rotating coherent features seen, those in the Gulf of Lion (Medoc Group 1970), and has been used ever since in many contexts, theoretical and observational, to describe such features, especially in winter when they are uniform right to the surface rather than being capped by a low-density summer water mass. Here the term *chimney* is preferred and it is important that uniformity should be introduced into the terminology used. This process can begin by tentatively defining a chimney as a “coherent submesoscale rotating vertical column, with uniform or near-uniform temperature–salinity properties extending from the sea surface (in winter) to depths far beyond the pycnocline.” Such a feature may appear to be like a subsurface eddy in summer when surface warming or advection caps it, but unlike a normal eddy, it opens up to the sea surface again in the subsequent winter.

Biological and chemical aspects

The data set acquired by ESOP on carbon cycling within the context of these deepwater formation processes not only confirmed that the Greenland Sea is probably a net sink for atmospheric carbon throughout the entire year (Skjelvan et al. 1999, Hood et al. 1999), but also began to provide insight into how the biological and solubility carbon pumps interact in modern high-latitude oceans. The results from the coordinated hydrographic, chemical, and biological studies indicate that biological processes occurring within the Greenland Sea play a minor role, compared with simple cooling, in setting the surface water CO_2 underpressure (Skjelvan et al. 1999). However, any possible causal relationship between the observed biological pump inefficiency and sluggish deepwater formation remains to be confirmed through studies in the presence of deep convection.

A synthesis of CFCs and inorganic carbon (i.e., dissolved inorganic carbon, pH, and alkalinity) data from the deep waters of the central Greenland Sea showed that in 1994–95, Greenland Sea Deep Water was composed of only about 80% convected surface waters from the same area, with the remaining 20% derived from the deep waters of the Eurasian Basin of the Arctic Ocean, which are low in anthropogenic carbon (Anderson et al. 2000). Although at this point it is unclear just how much these relative percentages shift as the strength of deep convection in the central Greenland Gyre waxes and wanes, a reduction in the rate of deepwater formation from the surface waters of the Greenland Sea will certainly reduce the rate of anthropogenic carbon removal into the deep ocean.

While the likely direct relationship between the efficiency of the solubility pump and deepwater formation rates has not been controversial, speculations on the nature of biological export in the source waters for deep convection have been distinctly contradictory. Some of the ideas that have been generated include that these areas would behave like other pelagic regimes, with high recycling and low export rates; that export should be enhanced in these regions because of the high seasonality of primary production due to the variations in light levels and ice cover; and that deep convection could carry fresh, labile dissolved organic carbon (DOC) to depth before remineralisation. Therefore, additional ESOP studies investigated the seasonal cycles of dissolved organic (Børsheim & Myklestad 1997) and inorganic (Miller et al. 1999) carbon, as well as sedimentation rates at 200 m (Noji et al. 1999). These three papers indicate that nearly all of the organic matter produced or released into the surface waters, including organic carbon released from melting sea ice entering the region through the Fram Strait (Gradinger et al. 1999), is regenerated at shallow depths rather than exported. Indeed, sedimentation of biogenic carbon is no greater in this region than in subtropical oligotropic gyres. All of the carbon transport rates observed during ESOP studies could conceivably change with various climatic factors, and it would be necessary to identify such correlations in order to draw any conclusions about how the ESOP findings may be dependent upon the rather special hydrographic conditions (low ice volume and low deepwater formation rates) at the time. For example, data from 1996 and 1997 indicate that although the average air–sea gradient in CO_2 during that time was larger than that during the ESOP study (Skjelvan et al. 1999), the actual flux across the air–sea interface may not have been any greater, and was possibly even less, due to the increased ice cover (Hood et al. 1999). Providing what may be a valuable tool for efforts to focus future field studies and to predict changes in the biological pump efficiency in the Greenland Sea, Slagstad et al. (1999) incorporated numerical chemical and biological carbon cycling models into a hydrodynamic model of the Nordic Seas to create a unified ecosystem model.

Models for the convection process

The onset of convection

The classic view of open-ocean convection (e.g., Killworth 1983, Marshall & Schott 1999) is that to predispose a region for convection there must be strong atmospheric forcing (to increase surface density through cooling or sea ice production), and existing weak stratification beneath the surface mixed layer (e.g., in the centre of a cyclonic gyre with domed isopycnals). One cause of the decline in Greenland Sea convection has been assumed to be global warming, causing an increase in air temperature and thus a reduction in thermal convection. The reduced convection could produce a reduction in the occurrence and growth of frazil–pancake ice in the Odden ice tongue, which used to form over the region every winter, and a positive salt flux through ice formation followed by advection (Wadhams & Wilkinson 1999, Wilkinson & Wadhams 2003). Another, possibly related, cause is that during the 1990s, with a positive North Atlantic Oscillation index, the occurrence of warm easterly winds over the region increased, reducing the occurrence of Odden and enhancing the decline in convection volume and depth.

There have been many attempts to describe and model the open-ocean convective process by which deep water is produced in the Greenland Sea. Most attempts were hampered by the fact that the actual convecting structure had never been observed, partly due to the difficulties of observation during the winter. The first models (Nansen 1906, Mosby 1959) featured a massive gradual overturning, whereas Clarke et al. (1990) proposed a convective adjustment approach. Killworth (1979) was the first to propose mesoscale chimneys as an analogy to chimneys that had been observed in the Mediterranean and Weddell Seas, and Häkkinen (1987) proposed an upwelling initiated by ice edge processes. Double diffusive convection processes were proposed by Carmack & Aagaard (1973) and McDougall (1983), whereas Rudels (1990) and Rudels & Quadfasel (1991) proposed a multistep process involving freezing.

Salt flux models

A salt flux model that incorporates ice formation, advection, and melt, as well as time-dependent brine drainage from frazil–pancake ice, was developed for the central Greenland Sea in winter (Wilkinson & Wadhams 2003) to test whether salt added by local freezing might be sufficient to trigger convection, as proposed by Rudels et al. (1989). During winters up to 1997 the tongue-shaped Odden sea ice feature sometimes protruded several hundred kilometres in a northeast direction from the main East Greenland ice edge and occupied the region influenced by relatively fresh polar surface water of the Jan Mayen Current (Figure 1) (Wadhams 1999, Wadhams & Wilkinson 1999, Comiso et al. 2001). The extent or shape of the Odden in any one year was governed by the limits of this freshwater layer as well as by surface air temperatures and winds, which vary on a daily basis because of the position of the Greenland Sea with respect to weather systems (Shuchman et al. 1998). This polar surface water layer is beneficial for ice formation, as only a limited depth of water needs to be cooled to freezing before ice formation can be initiated. As the Odden evolved, a bay of open water, known as Nordbukta, was often left between the Odden and the main East Greenland ice edge. In some winters, however, the Nordbukta froze and the Odden took the appearance of a bulge, and occasionally it forms as a detached island off the East Greenland ice edge. Fieldwork in the region showed that Odden consists primarily of *locally produced* pancake and frazil ice (Wadhams & Wilkinson 1999). Visbeck et al. (1995) was the first to measure ice motion in the region through Acoustic Döppler Current Profiler (ADCP) measurements. A set of specialised buoys, designed to mimic the motion of pancake ice, was then deployed within the Odden region in 1997 (Wilkinson et al. 1999). Comparisons between these buoys and European Centre for Medium-range Weather Forecasts (ECMWF) wind data showed that pancake ice within the Odden moves slightly to the right of the prevailing wind in a state of free drift, with a well-defined turning angle and wind factor that are a function of ice concentration. As the wind blowing over the Greenland Sea gyre during winter in the 1990s was predominantly from the north and west, any ice formed in the northern regions of the gyre was blown generally south and east. Therefore, the Odden can be thought of as a latent heat polynya, with wind blowing the newly formed sea ice away as it forms, adding salt at the surface.

The mechanism for salt-induced overturning would involve cooling as well. One mechanism is as follows. As winter approaches the initial surface cooling produces a homogeneous, near-freezing mixed layer (Visbeck et al. 1995). As the mixed layer approaches freezing the pycnocline between it and the Atlantic-based water below is further eroded. During most winters the surface water is cooled to such an extent that ice formation, i.e., an Odden, occurs in the region. The consequent brine rejection increases the density of the surface layer and has the effect of deepening the mixed layer (Visbeck et al. 1995). This entrainment of Arctic Intermediate Water combined with brine rejection produces a steady increase of the salinity and temperature (although this is lost to the atmosphere) of the mixed layer (Roach et al. 1993). As ice is blown away from the area, due to the prevailing northwesterly winds, more ice is formed, thus leading to further entrainment of AIW. During the mid- to late winter in some years the Nordbukta embayment opens up even though the southern and western rims of the gyre still have substantial ice covers. With the central region now ice-free, atmospheric surface cooling continues unabated and the mixed layer deepens further. Rapid deepening has been shown to be associated with strong wind outbreaks from the north (Schott et al. 1993). Due to the overwhelming entrainment of AIW, the Nordbukta remains open for the rest of the season despite surface cooling. The entrainment of AIW increases the density of the mixed layer until it reaches a point where deep convection can begin. An alternative mechanism involves the salt flux generating convective plumes that penetrate the pycnocline, a process discussed in the next section.

The salt flux model developed by Wilkinson & Wadhams (2003) was a semidiagnostic approach to the problem of estimating the contribution of salt flux to density enhancement in the winter Greenland Sea. The basic building block was Special Sensor Microwave Imager (SSM/I) ice concentration data, calculated according to a version of the Comiso bootstrap algorithm optimised for the Greenland Sea (Toudal 1999). The model has a time step of 1 day. The ice distribution given by the SSM/I map for day 1 was advected by the model into a new position for day 2, using wind velocity data from ECMWF and ice response (wind factor, turning angle) parameters derived from the buoy-tracking experiments (Wilkinson et al. 1999). The resultant ice map was compared with the real SSM/I map for day 2, and the difference ascribed to ice growth or melt. It was necessary to make plausible assumptions about the thickness of the ice and the quantity of brine released during the formation, ageing, and melting process. Data from various ESOP field experiments to the region (Wadhams et al. 1999) enabled empirical relationships for brine drainage rates as well as growth rates for pancake ice to be developed. In this way a daily salt flux was calculated from the difference between observed and advected ice. The model allowed for continuing brine drainage from the growing and ageing of the frazil–pancake ice, again based empirically on data collected during ESOP from actual pancakes retrieved from the sea and analysed *in situ* (Wadhams et al. 1996). When the model requires ice melt to occur in a pixel, the youngest (i.e., most saline) ice class in that pixel is melted first.

In March 1997 an intensive study of ice conditions within the Odden was performed by RV JAN MAYEN, during which pancake ice thickness and salinity measurements at 21 different locations within the Odden were obtained (Wadhams & Wilkinson 1999). This data set was used to verify and train the model, which was then used to estimate salt flux through the 1996–97 winter. Figure 5 (see colour insert) displays the calculated change in surface density through the winter due to this salt flux along a section at 75°N, assuming that the salt is distributed evenly over a mixed layer of 200 m depth. The surface density calculation assumes that the sea surface temperature is always at its freezing point (according to its salinity) and the ocean's initial salinity was 34.75.

These results were extracted from the model predictions of changes at 75°N 4°W during the 1996–97 winter and compared with actual observations made by a moored conductivity temperature depth probe (CTD) (at 50 m depth) deployed at that location by Budéus (1999). Figure 6 (see colour insert) shows that through most of the winter the observed change in salinity of the surface water gives a good match both in sense and in magnitude with the modelled change, indicating that the model is realistic and that salinity changes due to ice formation and movement dominated the surface water modification. In April 1997 a large excursion occurred, an increase in observed salinity unmatched by the model, but this also corresponds to a large increase in surface water temperature, from –1.8 to –1.4°C. It is likely therefore that at this time there was an intrusion of Atlantic water into the region.

The conclusion is that salt refinement is an important factor in preparing surface water for convective overturning, and that the magnitude of this refinement can be successfully modelled.

However, this leaves unanswered the question of how convective overturning occurs during winters in which no Odden forms (there was a partial formation in 1998 and nothing since), especially because these recent winters have been warmer than usual. Another salt flux model that works in a similar way, but with a different parameterisation for ice thickness, was described by Toudal & Coon (2001).

Plume models

The problem of how a surface density flux, whether induced by freezing or by cooling, is translated into convective motion was dealt with using a high-resolution, rotational, nonhydrostatic coupled ice–ocean model by Backhaus & Kämpf (1999). Typical initial conditions were applied representing mixed-layer situations in the central gyre region in early winter, and the model applied as a vertical ocean slice. The focus was on the initial penetrative phase of convection covering small (submeso) spatial and temporal scales, occurring after the imposition of outbreaks of strong atmospheric forcing, e.g., due to polar lows or other flows of cold polar air over the experimental region.

Model experiments were done on the erosion of a shallow (40 m) and of a deeper (100 m) cold, low-salinity surface layer such as occurs at the end of summer due to intrusion of meltwater from the East Greenland Current. The ice–ocean convection model utilised a grid size of less than 20 m and a thermodynamic scheme for ice growth that differentiated between frazil and pancake ice. A typical simulation would involve imposing a wind of 5 m s^{-1} at an air temperature of –20°C for 84 h (a typical polar low outbreak), followed by a more moderate continued cooling, with the ocean surface starting near the freezing point. The intense cooling phase produces an initial sea–air flux of 600 W m^{-2}, which diminishes as ice grows. In such a simulation a series of plumes develops, typically two or three per linear km and each of 100–200 m diameter. They increase in depth and after 48 h are penetrating the stratification at 200 m depth. Between the descending plumes warmer water is rising. With even more intense forcing (1000 W m^{-2} for 140 h) the convection reaches 1200 m depth. The rising warm water may cause the sea ice layer to melt or not, depending on initial conditions, so that haline and thermal effects may alternately dominate.

A steady-state model of a single plume was used by Thorkildsen & Haugan (1999) to show that such a plume could achieve penetrative convection to a depth of 1500 m. Its diameter, a few hundred metres, is greater than that of plumes that develop in the model runs of Backhaus & Kämpf (1999).

Direct observations of plumes are lacking, but the presence of plumes of approximately the appropriate diameter can be inferred from observational evidence obtained by Uscinski et al. (2003) in acoustic shadowgraph studies carried out over the Vesterisbanken in the Greenland Sea during the winter of 2001–2. An acoustic source and two receivers were placed 2.5–4.25 km apart, with transducers at depths of 140–250 m, and the acoustic intensity pattern was interpreted as implying downward velocities of a few cm s^{-1} within distances less than the source–receiver distance. Further analysis of the data is still taking place.

Recent work

The impetus for a new series of observational studies in the region, to try to resolve both the nature and mechanism of open-ocean convection, came mainly from a new European Union research project, CONVECTION (contract EVK2-CT-2000-00058), together with domestically funded efforts by Norsk Polarinstutt (NPI), Alfred-Wegener-Institut für Polar- und Meeresforschung (AWI), and Institut für Meereskunde, University of Hamburg (IfM). The effort made to date (June 2003) and reviewed here has comprised winter and summer cruises for each of the years 2001 and 2002, together with a winter–spring cruise in 2003. Subsequent reference to the cruises will be abbreviated to W01, S01, W02, S02, and WS03.

Winter 2001: JAN MAYEN and LANCE

In winter 2001 two cruises took place to the central Greenland Sea gyre. The first, by Institut für Meereskunde, University of Hamburg, used RV JAN MAYEN for a study of the central gyre region during March 12–26. The second, a cruise of the EU CONVECTION project, used RV LANCE for a resurvey of the same region 1 month later (April 11–24).

During the first cruise in 2001 JAN MAYEN carried out a section at 75°N starting from 10°E. In the vicinity of 0° a chimney-like feature was discovered that was investigated by a network of closely spaced stations during March 22–23. Figure 7A (see colour insert) is a contour map of the depth of convection. To generate this figure we define the depth of convection at a given station as the depth over which the potential density σ_θ remained constant and did not increase more than 0.002 kgm^3 above its median value in the 200- to 600-m-depth range. The centre of convection, inferred from contouring of the station data, was at 74° 56.9'N, 0° 23.5'E, with a convection depth of 2430 m; the convection depth of the deepest individual station (no. 80) was 2426 m. Given the role of thermobaricity in affecting the density profile (Garwood et al. 1994), it is more accurate to speak of the "depth of the well-mixed layer" than the "depth of convection." Nevertheless, it is clear from profiles such as station 47 in Figure 13 (see colour insert) that the depth defined refers to a water column that has uniform temperature and salinity properties.

In April LANCE returned to the position identified as the centre of the feature by JAN MAYEN and began a survey that accomplished a S–N section and most of an E–W section before being broken off due to weather. The ship returned to the area later in the cruise (April 20–22) and initiated and completed a fresh survey (Figure 8, see colour insert), of which the results are shown in Figure 7B. From the temperature, salinity, and density profiles the location of the deepest convection was identified as station 10 in leg 1 and station 47 in leg 2, which was at 74° 56.8'N, 0° 24.9'E. If it is assumed that these stations represent the centre of the chimney, then this centre moved approximately 5 km due north between legs 1 and 2, during a single week, while the net movement between mid-March and mid-April was only 710 m to the east (093°). The positional data showed that the chimney has two dynamic properties: it remains within a very circumscribed region and it moves within that region at a rate that makes it necessary to carry out any closely spaced CTD survey rapidly, within a day or two, in order to define the very tight structure without time-dependent "smearing." In fact, the apparent movement between March and April, tiny as it was, may be an artefact of the contouring process from a finite set of stations, or could be affected by errors in the effective positioning of each station (the Global Positioning System (GPS) position used for each station was an average position during the cast concerned, which took about an hour, during which time the ship drifted). Thus, it cannot be said with certainty that the feature moved at all, but it is likely that the movement, if any, was remarkably small. The interpolated depth of convection at the centre of the feature was 2460 m (maximum individual station depth of 2520 m), which is similar to the 2430 m observed by JAN MAYEN, so the two cruises demonstrate that the feature possessed a remarkable stability in location, shape, and depth.

From this LANCE survey Figure 9A and B (see colour insert) show E-W salinity and density sections across the centre of the feature, while Figure 9C is an E-W potential temperature section from JAN MAYEN done slightly farther north at 75°N, and so is missing the very centre, but covering a wider range of distance and depth. It can be seen that a second, smaller capped feature appears to exist some 60 km W of the main feature, while the main feature appears to have pushed the underlying temperature maximum downward rather than just penetrating through it. The uniformity of the water column within the feature is clear from Figure 9, as is the abruptness of the convection limit.

The contour plots show not only that this is the deepest convection recorded in decades, but also that its spatial scale is of particular interest. The region of deep convection, i.e., greater than 2000 m, is tightly contained within a 5-km radius. Within this radius there is vertical homogeneity in the water column as can clearly be seen by comparing the hydrography from LANCE station

28 with that from station 47 (Figure 13). Hydrographic measurements performed at station 28 reveal a strong pycnocline at around 1300 m, but less than 20 km away homogeneity is present in both potential temperature and salinity and hence density until approximately a depth of 2400 m. The feature is identified as a chimney using the definition developed earlier and used by Killworth (1979) for modelling and by authors such as Sandven et al. (1991) for the results of observations.

Closer examination of the hydrography surrounding and within the chimney highlights some very interesting features (Figure 9, Figure 12, and Figure 13, see colour insert). The potential temperatures within the chimney are colder than –1.0˚C, whereas the surface waters outside the convective region have temperatures above –0.9˚C. The salinity is also lower within the chimney (<34.87) than the surrounding water, but of particular interest is the water density (σ_θ) within the chimney (Figure 9B). The surface waters inside the chimney are denser than the surrounding stations, as one would expect within a convective region; however, this appears to reverse beyond 1500 m. Taking account of thermobaricity, an analysis of baroclinic pressure differences shows that in fact the pressure outside the chimney does not exceed the pressure inside at the same depth until 2000 m is reached (R.W. Garwood, personal communication). It can be seen from Figure 9C that the layer of temperature maximum, located nearby at 1800 m, occurs some 500 m deeper under the chimney.

Figure 9C also demonstrates two interesting aspects of the central gyre region surrounding the chimney. First, there is a temperature maximum (T_{max}) layer in the region of 1500–2000 m depth; there is evidence (Budéus et al. 1998) that this is a relatively recent feature of the water structure in this part of the Greenland Sea, having developed in the late 1980s and steadily deepened since, from 800 m in 1993 to 1500 m by 1996, although recently this deepening has slowed or ceased. Annual overturning of the water column has not eroded the T_{max} and it is only water above the T_{max} layer that has been modified by convection induced by atmospheric and sea ice forcing. Underneath the chimney the layer is displaced downward as if it had been pushed down by the presence of the chimney. This behaviour resembles that of a chimney observed in the Labrador Sea in 1976 (Clarke & Gascard 1983, Gascard & Clarke 1983), in which a 2200-m-deep chimney appeared to have pushed down the North Atlantic Deep Water (NADW) underneath it, while around it this water mass was found at 1500 m depth.

Second, there is evidence of a second structure to the W of the main chimney (at station 22). This has similar width to the chimney (although the station spacing makes this an approximate observation), and has also “pushed down” the temperature maximum to a depth of about 2000 m. However, it is capped by warmer near-surface waters. It is tempting to identify this structure as the remnants of an older chimney that is no longer active, and where shallow waters have moved in and eliminated its upper structure, but it is also possible that it is a chimney in the process of formation or, as suggested by J.-C. Gascard (personal communication), a subsurface eddy that may later open up to the water surface if and when intense surface cooling takes place.

Finally, Figure 10 (see colour insert) provides a graphic illustration of the remarkably symmetrical cylindrical shape and tightly constrained structure of the chimney by showing a three-dimensional view of the –1.0˚C potential temperature surface (red) as it displaces the warmer water (–0.9˚C surface, yellow), which underlies the cold surface water in the region immediately surrounding the chimney.

The evidence from the 2001 winter measurements showed that rotating chimneys can extend down to depths characteristic of deep convection, but their role in deepwater renewal is less clear because, at least in this case, the deep core of the chimney is less dense than the surrounding water, besides appearing very stable. The equilibrium depth of the water inside the chimney is <1800 m. Therefore, it is not clear whether active ventilation down to the full 2500 m is occurring within the chimney, nor whether, when the chimney collapses, there will be significant output of convected surface water at the 1800- to 2500-m level.

Because sea ice did not extend to this region in 2001 (or in 1998–2000) the origin of the chimney had to be surface cooling rather than salinity enhancement, unless the chimney was at least 4 yr old.

The origin of the rotation was also a mystery: it could have been induced by the act of convection, or there is a possibility that the chimney was spun up by some kind of flow over the surrounding seabed topography. Figure 11 (see colour insert) shows the chimney location from W01 in relation to the local bathymetry. The chimney lay over a smooth bottom of depth of about 3600 m, but only 30 km to the NE the seabed rises to a ridge (the Greenland Fracture Zone) less than 2000 m in depth. This ridge runs SE from the edge of the East Greenland shelf, and it seemed possible that some deep flow from the East Greenland Current was diverted along it, creating instability as water crosses the ridge crest (e.g., through the gap NE of the chimney) to return to its southward geostrophic path. As will be seen later (p. 22), later experimental data do not support this hypothesis.

The temperature structure of the chimney can be seen in more detail from LANCE W01 results. Figure 12 (see colour insert) shows N–S sections through the chimney from leg 1 and leg 2. Of particular interest is the region of cold water (–1.04°C), which is confined to the centre of the chimney. Surrounding the cold column of water is a wider region of slightly warmer water (–1.02°C), which fills up the rest of the chimney. Outside the chimney the water is still warmer. Vertical profiles of potential temperature (Figure 13) for the chimney centre (station 47) and the nearest stations to it (31, 45, 48, and 49, all 5.6–6.3 km away) show that the temperature profile at the very centre is uniform, evidence of complete mixing to the full depth of convection, while the temperatures elsewhere in the chimney still show fine structure and a generally negative gradient with increasing depth, indicating that cooling and mixing are still going on. From these results we infer that the central core of the chimney is limited to less than 5-km radius around the centre. Gascard et al. (2002) showed that this is the radius within which the chimney rotates as a solid body, with slower rotation outside this. Thus, either temperature or rotation rate could be used as a criterion to define an effective diameter for the chimney, a third criterion being the diameter of the region where the T_{max} layer has been displaced downward. From Figure 9 and Figure 10 this zone of displacement appears to be 20 km across, suggesting an inner core of 10 km maximum diameter and a skirt, or outer zone, of 20 km diameter.

Summer 2001: LANCE

An APEX float was placed at the chimney centre in spring 2001 by D. Quadfasel (University of Copenhagen), drifting at 1000 m depth and carrying out a T,S profile from 2000 m to the surface every 10 days. The float data assisted the rediscovery and resurvey of the chimney by LANCE during October 2001. The survey began on October 10 at station 24 (Figure 8B), at which the intermediate and deeper waters showed the same structure as in the winter, but with a fresher cap at the surface. With the weather good, the whole chimney was resurveyed.

Figure 8B shows the station map; stations 24–42 are within the chimney, and all stations were carried out during the period October 10–13, 2001. There were 18 stations covering the region of influence of the chimney, both the inner core and the outer zone, with station 39 (74° 53'N, 0° 17'E) assumed to be closest to the chimney centre on account of having the greatest depth of convection. Stations 42 and 43 are more distant to the E.

The location of the chimney and the contours of convective depth are shown in Figure 14 (see colour insert) in relation to W01 (and to the later W02). Figure 14 shows that the chimney centre moved a net 8.2 km in a SW direction (204°) between April and October 2001. Convective depth was defined as it was for the winter 2001 data (the depth over which the potential density remained constant and did not increase more than 0.002 kg m^{-3} above its median value in the 200- to 600-m-depth range) except that the reference depth range was 800–1500 m so as to get below the capping layer. The contours show that the chimney was of almost identical shape, and reached an identical depth, to that in April 2001. When the data from the APEX buoy are also considered (Wadhams et al. 2004a), which show continuity of the T,S structure, it is clear that there is continuity between the chimneys of April and October 2001; i.e., it is the same feature rather than the replacement of one chimney by another.

Figure 15B (see colour insert) shows a potential temperature section (W–E) through the centre of the chimney region, while Figure 16B (see colour insert) shows salinity and Figure 17B (see colour insert) potential density. The chimney is clearly visible in Figure 15B, with the deep temperature maximum depressed below it, as seen the previous winter. It is dramatically clear that the lower part of the chimney, below 500 m, has remained unchanged in shape and temperature since the winter, whereas the uppermost 500 m has been influenced by the surrounding water. This influence takes the form of a surface layer of warm water, around 3˚C and approximately 50 m thick, which has established itself during the interval between the summer and winter cruises and which is now capping the chimney and preventing active convection. It is likely that the source of this water is melt of sea ice from the East Greenland Current to the west, which has produced a low-salinity surface water mass that has spread out over the Greenland Sea, either laterally from the East Greenland Current or via the Jan Mayen Current, so as to produce a summer capping. In addition, between 50 and 500 m, a warm, higher-salinity subsurface water mass has spread laterally into the flanks of the chimney, narrowing it so as to produce a rounded lid to the water volume, which in winter had constituted the chimney's core. Figure 18A (see colour insert) shows these near-surface modifications in detail.

Figure 19A (see colour insert) compares the temperature structure at the assumed centre of the chimney (station 39) with the four nearest surrounding stations (24, 25, 28, and 31, at 5.3–6.9 km from centre) and to the more distant station 38, 15 km away. The following immediately apparent features are of interest and importance.

1. *A deep temperature maximum that is pushed down below the chimney centre.* Underneath the five core stations the temperature maximum is –0.92 to –0.94˚C, occurring at depths of 2500–2800 m. Around the chimney core there is a shallower temperature maximum layer, with a peak (for station 38) at –0.83˚C and 1600 m depth. The chimney pushes the maximum down and cools the temperature maximum layer, although between this peak and the seabed the temperature is higher than in the region surrounding the core. This behaviour of the deep temperature maximum was also observed in winter.
2. *An unchanged chimney core extending from about 1500 m down to the convection limit.* Within this range the temperature is –1.04˚C as it was in winter 2001.
3. *Detectable intrusion of warmer water above 1500 m*, increasing greatly in temperature gradient above 500 m.
4. *A thin but extremely warm surface layer*, some 50 m thick and rising to +3˚C.

The salinity section through the centre of the chimney (Figure 16B) and salinity profiles from the above stations (Figure 19B) show that the warm surface water mentioned above also is less saline, which confirms its identification as Polar Water (PW) from the East Greenland Current. This water spreads over the central Greenland Sea during most summers; originally it is near freezing, but significant warming due to solar heating during the summer raises the temperature. Below this layer higher-salinity water occupies the chimney down to about 500 m, after which the salinity is almost homogeneous until it reaches the temperature maximum, 1500 m, where it begins to increase again in the water (station 38) surrounding the chimney. Because the chimney has displaced the waters of the temperature maximum, the homogeneity in salinity (34.88) extends to 2500 m within the chimney centre and 2100–2300 m elsewhere in the chimney.

A potential density section through the chimney region is shown in Figure 17B (full depth) and Figure 18C (uppermost 500 m), while Figure 19C shows density profiles from inside and outside the chimney. For the region below 500 m these figures show very clearly the same general features as seen in the previous winter; i.e., the upper part of the chimney has more dense water than the surrounding waters (station 38) and the lower half of the chimney has less dense water. The effect of the warm freshwater cap on density can be clearly seen in Figure 18C. Within the chimney core (station 39), below the level of the cap, the changes in temperature and salinity offset one another and from 250–2500 m the potential density is constant within 0.001 kg m^{-3}. However, the other profiles in the outer zone show a density gradient that continues down to about 1000 m.

Note that the potential density profiles show that the waters within the core and outer zone of the chimney are less dense than the surrounding region below 1500 m (2000 m if thermobaricity is taken into account; Wadhams et al. 2002) and more dense above, but that the integrated density with depth is less within the chimney than outside it. The implication is that the water surface above the summer chimney centre should stand higher than its surroundings, so the chimney may be detectable as a bump when viewed by a satellite laser or radar altimeter that has a good enough horizontal resolution. Another way in which the chimney may be detectable by remote sensing is from a contrast in surface wave propagation at the edge of the chimney, as occurs in fronts (Fischer et al. 1999), giving a change in brightness on synthetic aperture radar.

Winter 2002: LANCE

In February 2002 LANCE surveyed the chimney for a third time (cruise W02) (Wadhams et al. 2004a). The weather was particularly bad throughout the cruise. The first station was performed on February 17 at the centre location of the chimney as seen in S01. The profile did not show a convective regime and a second station was performed farther east, also outside the chimney. Weather then prevented work in this region until February 28. The chimney was successfully relocated with the first station on that day, and a pattern of nine stations was carried out at approximately 6-km spacing within the chimney region until March 2, when bad weather prevented further station work during the cruise, despite the ship remaining on site until March 7.

Figure 8C shows the locations of the winter 2002 stations. Stations 1 and 2 were the initial stations carried out at the start of the LANCE cruise on February 17, 2002; they proved to lie about 12 km E of the chimney. Stations 27–35 constituted the grid of nine stations that it was possible to carry out on March 2–3. Stations 50–53 were stations carried out at our request by ARANDA on March 23 (chief scientist J. Launiainen, Finnish Institute of Marine Research). The hope was that the chimney would not move significantly during the intervening period; therefore, station 50 represented the best guess of where the chimney centre would be, while 51–53 represented stations required to complete the survey of the SW side of the chimney.

In the event, it is clear that the chimney moved substantially during the period between March 3 and March 23, as it did between the two LANCE surveys in winter 2001. Not only did ARANDA find no evidence of the chimney, but she also found no evidence of the regional convection that appeared to be occurring in the outer zone of the chimney down to some 1500 m. The important result is that the chimney was migrating during early March and that both the core and the outer zone lay outside the survey area of ARANDA on March 23.

Figure 14 shows the location of the chimney on March 3 and the convective depths, defined in the same way as before. Clearly the limited station grid succeeded in defining about two thirds of the chimney, leaving the SW corner unsurveyed, and we see that the chimney centre moved only a net 18.5 km to the NW (course 288°) between October 2001 and March 2002. Once again the chimney is displaying its tendency to remain within a very limited geographical region, as well as significant longevity. Figure 15C shows the potential temperature structure in a section across the chimney.

In Figure 20A (see colour insert) as before, we examine the potential temperature profiles for the assumed centre of the chimney (station 31) compared with three nearby stations in the outer zone (station 32, 5.6 km away; station 30, 6.0 km away; and station 27, 8.3 km away) and a more distant station (station 28, 13 km away). They demonstrate four key features, of which the first two are the same as in summer 2001:

1. *Deep temperature maximum that had been pushed down below the chimney.* This figure illustrates a temperature maximum that is about –0.85°C at 1800 m in station 28, being pushed down to 2600 m at –0.90°C in the other four stations. Figure 20A also shows that the colder value of T_{max} under the chimney was compensated by warmer temperatures between the T_{max} depth and the seabed, using station 28 as the control.
2. *A core region of the chimney that remained unchanged relative to both summer 2001 and winter 2001.* This is the region of uniform temperatures and coincides with the following depth ranges: 1700–2500 m, station 27; 1400–2400 m, stations 30 and 31; and 900–2000 m, station 32. The value of the temperature (about –1.04°C), and the maximum depth of convection (up to 2500 m), corresponded with the shape of the chimney as seen in Figure 15 which, in its deeper part, remained unchanged and untouched since winter 2001.
3. *A region where new winter convection appeared to be occurring, which had not yet reached a depth exceeding 1500 m.* This region appeared to extend down from 500 m until it met the long-term unchanged heart of the chimney. In some cases (e.g., station 27) a uniform temperature profile, albeit warmer than the chimney core, had been established; in others (30, 31, and 32) the temperature warmed toward the surface. Station 28 shows that this winter convection is in fact regional and extended outside the limits of the chimney core, because a uniform temperature profile of –0.94°C extended from 500–1400 m. It appears that the winter uniform structure had not yet been able to fully establish itself, because the 2002 survey was done earlier in the winter than 2001.
4. *A near-surface region of variable temperature.* From 500 m to the surface all five profiles show variable temperature structure, with 500 m being a distinct discontinuity, suggesting that the zone above 500 m is one in which infiltration by surrounding waters has occurred. It should be noted that this was the depth to which significant water mass infiltration had occurred in the October 2001 data.

Figure 20B shows the corresponding salinity profiles, in which the same four features can be seen, although the temperature profile is a better separator of water types. The deep temperature maximum becomes a broad salinity maximum, with station 28 having slightly lower salinities near the seabed than the other four stations (compensating for its lower temperatures). The core region is the same, except that the uniform salinity in station 32 extends slightly deeper, to 2100 m. The region of new winter convection has a salinity similar to that of the old core region, except for station 31, where it is distinctly higher, implying instability and a winter convection regime that must be actively increasing the convection depth; and station 32, where there is instability in the uppermost 500 m. The profiles of potential density (Figure 20C) follow mainly the shape of the salinity profiles and show the same sequence (moving upward) of warm deep layer, core of the 2001 chimney, and zone of new winter convection reaching down toward it.

By contrast, the ARANDA stations, from the same locations as the chimney stations of 3 wk earlier, show no evidence of any structure resembling the chimney core or outer zone. The temperature profiles all show a warm peak at about 1600 m, with no evidence of winter convection occurring above it, while the salinity profiles also show no evidence of a winter convective regime. Since there was no warm weather between March 3 and 23, so that any winter convection induced by cooling might be expected to have remained in place, it is clear that the entire chimney, comprising both the core and the outer zone, had advected out of the area within this 20-day period, to be replaced by surrounding water that had not undergone convection. This is similar to the process of migration-within-limits observed in winter 2001.

The profiles of Figure 20A show that the fine temperature structure in the core region of the chimney is smooth, while in the region nearer the surface where the winter convection regime is still establishing itself there is much greater small-scale variability. As noted in relation to W01 and S01 data, and as described by Galbraith & Kelley (1996), the high-frequency variability is a sign of active convection.

With respect to the depression of the T_{max} layer, the shape of the chimney has remained the same through W01, S01, and W02, but the waters within the chimney, both the core and the outer zone, have been modified. The outer zone and the shallow part of the chimney have been most susceptible to modification. This suggests that the chimney is evolving toward a state similar to that of the feature at station 22 in March 2001, i.e., supportive of the idea that the feature seen is indeed a relic of a chimney rather than a nascent chimney.

Summer 2002: POLARSTERN

The chimney was resurveyed by FS POLARSTERN in August 2002 with 22 CTD stations, vessel-mounted ADCP, and bacterial analysis (Budéus et al. 2004). It appeared similar in hydrographic structure to that in summer 2001, with a capping of less saline water. However, thanks to the ADCP its velocity structure could be defined properly for the first time. Direct ADCP measurements showed the velocity field in horizontal slices, e.g., between 150 and 200 m (Figure 21A, see colour insert), while the ADCP velocities at 400 m were used to correct geostrophic shear calculations and so produce a complete velocity cross section of the chimney (Figure 21B).

The measurements show that the anticyclonic velocity structure was symmetrical, with a maximum speed of 30 cm s^{-1} achieved at a depth of 2000 m. The speeds diminished toward the surface, where the maximum was about 15 cm s^{-1}. At any given depth the whole pattern was of a constant angular velocity, a rigid body rotation, extending from the centre to a radius of 9 km. Beyond this radius the angular velocity decreased until the chimney merged with its surroundings, where the rotation was modestly cyclonic. The 9-km-radius limit for constant angular velocity corresponded to a point where the isopycnals, which were approximately horizontal outside the chimney, took on their steepest slope in descending toward the chimney centre. The azimuthal speeds imply a rotation period of about 40 h at 2000 m and a relative vorticity of $-f/2$, similar to the value found by Gascard et al. (2002). Rotation periods above and below this depth were somewhat greater, yielding a vertical velocity shear that in theory should dissipate energy from the high-speed core of the chimney. In practice this did not seem to occur, and an enduring mystery of chimneys is their long-term ability to retain angular momentum, requiring a recharging mechanism to replace that lost by dissipative processes.

The bacterial analysis suggested that exchanges between the interior of the chimney and the background are slight. In the Greenland Sea in general, bacterial abundance decreased rapidly with increasing depth, from 9×10^5 cells ml^{-1} near the surface to 8×10^4 cells ml^{-1} at 600–1000 m and 4×10 cells ml^{-1} below the temperature maximum layer. However, inside the chimney the abundance remained at about 8×10^4 cells ml^{-1} down to 2500 m. This is evidence for a surface-to-depth link within the chimney whereby plankton-rich surface waters reach deep levels by winter convection, but not a strong lateral link between the chimney and its surroundings at any given depth. One expects, therefore, that plankton and nutrients as well as bacterial biomass would be transferred to depth from the surface in this way.

Winter–Spring 2003: POLARSTERN and LANCE

In April–May 2003 two further cruises took place in the region (Wadhams et al. 2004b). In the first, by FS POLARSTERN, the 75°/0°chimney was rediscovered very close to its original location and remapped. In the second, by RV LANCE, the same chimney was found to have moved 28.4 km to the northward (bearing 5.6°) in 27 days while retaining an identical structure. At the same time, a systematic grid survey of the entire central gyre region revealed that one other, and only one other, chimney existed in the region of the gyre centre, some 70 km to the NW of the 75°/0°chimney (Figure 22, see colour insert).

These remarkable results demonstrate that the 75˚/0˚chimney is not a unique phenomenon, generated by some site-specific mechanism, but is one member of a class of features found in the central Greenland Sea gyre and similar to structures seen in the few other regions in which open-ocean convection occurs in winter, i.e., the Gulf of Lion, Antarctica, and the Labrador Sea (Marshall & Schott 1999). The fact that only two chimneys currently exist in the survey region (and thus only perhaps two to four in the entire Greenland Sea gyre) shows that chimneys are not common and that it is difficult to create a chimney.

Figure 22 shows the central Greenland Sea gyre region, together with the station grid occupied by LANCE during May 19–30 2003, which was designed to cover the whole of the central gyre region that was especially susceptible to overturning because of domed isopycnals. The grid spacing was 10 n ml (18.5 km) which is slightly less than the overall diameter of the 75˚/0˚chimney. It was therefore deemed unlikely that a chimney could exist within the grid area and not be detected by some departure of the station from a conventional regional T or S profile. The figure shows the location of the 75˚/0˚chimney as discovered by POLARSTERN on April 27, when it was centred at 74˚ 50.5'N, 00˚ 03.5'W. LANCE went to this location for her first station, but no trace of the chimney was found here or in a widening search pattern of 21 stations. After the grid survey was begun, however, the chimney was detected at a grid point and its centre and structure defined by a further series of closely spaced stations. The new position of the chimney centre, on May 24, was 75˚ 11.0'N, 00˚ 4.3'E. This means that the feature had moved a net distance of 28.4 km on a bearing of 5.6˚ in 27 days, a speed of 1.05 km day^{-1}.

Figure 23A (see colour insert) shows the temperature and salinity structure from two transects carried out across the chimney in NE-SW and NW-SE directions at 2.5 n ml (4.6 km) station spacing, drawn on the same scale as Figure 23B, which shows the structure of the POLARSTERN chimney. Clearly these are two surveys of the same feature. In fact, the similarity extends down to detailed features of the contour shapes, which is remarkable given the spatial displacement, the time delay, and the fact that the transects were not necessarily in the same directions relative to the chimney's axes. The central core has a centre potential temperature of –1.02˚C and salinity of 34.895, which, as Figure 24 (see colour insert) shows, represents only a slight drift from its core properties in previous seasons and years. In addition, in both April and May the chimney core was covered by a dome of warmer, less saline water. It is not clear whether this represents the beginning of the summer capping, as observed later in the summer in 2001 and 2002, or whether this indicates that the chimney did not reopen completely to the surface during the winter of 2002–3, which may have implications for its continued survival.

On May 30 the chimney was found again. The position of the centre was now 75˚ 13.4'N, 00˚ 20.8'W, indicating a distance of 12.7 km in 6 days (2.1 km day^{-1}) on a bearing of 290˚. Figure 25 (see colour insert) shows the T profile of the station thought to be over the centre of the chimney core as compared to the station at the core centre on May 24. The almost identical profile shape shows that the centre was indeed successfully located and that once again the feature was maintaining a constancy of structure. The drift direction and speed, however, had changed. If the chimney's trajectory is compared with that of the APEX float which was deployed in the chimney in March 2002 at a depth of 1000 m (but which rapidly left the chimney that at that time was stationary), it can be seen from Figure 22 that during April–May 2003 the chimney was following the trajectory of the intermediate water in the region rather than staying in virtually the same position as it did from 2001 until this year. It is possible, therefore, that the chimney may have been in the process of advecting out of the central gyre region.

Elsewhere the grid survey revealed the presence of a second chimney (chimney 2) that was centred at 75˚ 34.0'N, 01˚ 47.9'W, a position shown on Figure 22. This chimney was also capped and had a cold core structure similar to that of the 75˚/0˚chimney. However, the core potential temperature was somewhat higher, at –0.96˚C instead of –1.02˚C, while the core salinity was similar at 34.895 and the potential density also similar at 28.065. This interesting result suggests a different method, date, or location of formation, and shows that not all chimneys are the same and that we can identify a chimney by its core characteristics. Figure 26 (see colour insert) shows the temperature, salinity, and density structure of the chimney, and it can be seen how the shape agrees with that of the 75°/0°chimney. It was not possible to make a later repeat survey of chimney 2 to see how fast it was moving.

Away from the chimneys the water structure in the central gyre region in April 2003 was very consistent over the whole grid area. A characteristic as usual is the T_{max} layer at about 1500–1800 m. The effect of the chimney is to displace the T_{max} layer to 2200–2700 m, below the base of the chimney, and in so doing, to displace all the lower water masses so that the bottom temperature under the chimney increases, the warm shadow effect. This T_{max} layer depression was used as a test for the propinquity of a chimney in analysing grid stations. Another characteristic of a chimney is that the core temperature, at –1.02°C for the 75°/0°Chimney and –0.96°C for chimney 2, is significantly colder than the minimum temperature reached at mid-depth in a conventional station, typically –0.85 to –0.90°C. This in itself is evidence that the chimney's origin involved cooling. Thus a virtue of the regularity of structure in the mid-gyre is that it enables deviations due to the influence of a chimney to be readily recognised. Hence one can be confident that if there are more than two chimneys in the Greenland Sea, the additional unseen features lie outside the 15,000 km^2 of the grid shown in Figure 22, although this is unlikely because the water structure is more stable away from the gyre centre.

Implications of recent work

The seasonal evolution of a chimney

For this analysis the most informative Figures are 15–17 and 25, in which potential temperature, salinity, and potential density sections across the successive states of the chimney are compared. The most obvious conclusion from these figures is that the deep core of the chimney remained remarkably constant in shape, temperature, and salinity throughout the five seasons.

The upper waters of the Greenland Sea show considerable variability both seasonally and annually (Bönisch et al. 1997), and the data set displays significant changes in both temperature and salinity in the 6-month period between the W01 and S01 cruises. These changes are most pronounced in the upper 50 m where a lens of warm (~3°C), relatively freshwater (34.765) spreads over the surface of the gyre and, in doing so, caps the chimney, insulating its waters from direct heat exchange with the atmosphere. This freshwater lens covers the gyre most summers and originates from the Polar Water (PW) of the East Greenland Current. Whether this water is transported into the gyre region via the Jan Mayen Current (~73°N) or has spread out from the EGC farther north is open to debate; during its passage, however, it has warmed so that it is no longer near the freezing point as it was when it emerged through Fram Strait.

There is also a possible role for local hydrological forcing (precipitation (P), evaporation (E)) in the evolution of the freshwater lens. A (P–E) of 17 cm over the intervening 7-month period would be enough to decrease the salinity from 34.885 (surface salinity in April) to 34.765 (surface salinity in October) over a depth of 50 m. However, if we assume (P–E) is zero and the freshening is due to an influx of PW only, then approximately equal volumes of PW and local winter surface water would produce the summer cap water in a binary mix. In reality, both processes must be occurring, and if at some stage more saline Atlantic water entered the region, then more precipitation or PW is needed to achieve the salinity of the summer cap.

Figure 27 (see colour insert) is a T,S diagram that shows the surface water properties of the summer cap (blue star) at station 39 (centre of chimney) with their variation with depth down to 300 dbar. Also shown in the figure are the surface water properties of the EGC as seen in winter 2001 (green star, from LANCE W01 cruise) and the central chimney station (station 47) as seen in winter 2001 (red star). From this figure it can be seen that waters below the uppermost 50 m of the summer cap are slowly approaching the water properties of the winter chimney. A mixture of approximately equal parts of EGC surface water and chimney core water, if heated by approximately 4˚C, could account for the chimney surface cap.

Below the summer cap the regional water masses show some variation in their properties between W01 and S01. At some time after W01 a water mass with increased salinity and temperature entered the region, modifying the waters between the bottom of the cap and 650 dbar (see Figure 15). Below 650 m the water properties remained essentially unchanged from winter.

Unlike W01 the summer profiles within the chimney show a distinct warming down to approximately 1550 m and an increase in salinity down to 650 m. These changes, which mirror the modification outside the chimney, can only occur by the exchange of water between the inside and outside of the chimney. Below 650 m no salinity gradient exists between the inside and outside of the chimney; thus exchanges below this depth only affect temperature. The water properties within the chimney remained unchanged below about 1550 m. This depth may be significant as it corresponds to the beginning of the temperature maximum. It is possible that the strong pycnocline between the temperature maximum and the waters above protects the chimney from the intrusion of water from the side. Furthermore, the infiltration of Atlantic-based water in the upper reaches, 50 to 500 m, of the chimney gradually modifies the water properties from the outside of the chimney toward the centre. The combination of the infiltration amount varying with depth and the rotation of the chimney produced the tapered top surface to the chimney. Below the chimney temperature maximum very little modification occurred to the waters. In both winter and summer the depression of the temperature maximum is still present; however, owing to the lack of CTD cable in winter 2001, we are unable to confirm if changes in the deep water occurred at the site under the chimney.

By March 2002 the warm layer had completely gone and the chimney reopened. This comprised the 50-m layer of polar meltwater of very low salinity and very warm temperature (about 3˚C) and also the deeper water between 50 and 500 m, which had a higher salinity than the subsequent winter water in the chimney (compare Figure 16 and Figure 18). The chimney was again active, although it had two distinct water masses in it now, upper and lower. The upper water mass was formed from 2002 winter's convection, the lower from the remnants of the water mass that was originally in the chimney in 2001. Thus between S01 and W02 the surface layer that capped the chimney eroded away. The question arises as to whether the upper water mass within the W02 chimney could have formed by the mixing down of summer water, modified by cooling. If Figure 16 and Figure 18 are compared, it appears as if this might be the case, as the low-salinity surface layer and the high-salinity peak at about 200 m look as if, when mixed together, they could generate the uniform salinity shown in Figure 16B. This is almost perfectly the case because the mean salinity of the uppermost 1500 m for the S01 centre station (39) is 34.877, while for the W02 centre station (31) it is 34.883. Therefore, it is possible to imagine that although the summer structure in the upper part of the chimney was created by the lateral advection and intrusion of other water masses, the subsequent transition to winter mainly involved these overlying water masses simply cooling, mixing vertically, and convecting down to 1500 m to join on to the deep surviving core of the chimney, creating a new composite winter chimney. As winter progresses, further adjustment would turn this composite chimney into one that is completely uniform down to maximum depth.

Possible fate of water from chimneys

An APEX float was deployed at the assumed centre of the chimney, 74˚ 59'N, 00˚ 09'W, on March 6, 2002. The float was designed to descend to 1000 m (parking depth), then every 10 days to sink to 2000 m and rise to the surface, recording a temperature–salinity profile that was then transmitted by satellite during a 6-h surface sojourn. Such a float had been deployed in the same chimney in spring 2001 by D. Quadfasel (University of Copenhagen) and remained within the chimney until February 2002. The present float appeared to leave the chimney quite quickly and has since been participating largely in the cyclonic circulation of the general gyre centre (Figure 28, see colour insert), including a NW transect following the side of the Greenland Fracture Zone. The float therefore tells us nothing useful about the recent development of the chimney, although the motion (shown in an inevitably jerky fashion since points separated by 10 days of drift at 1000 m are connected) may contain an eddy-like element since the trajectory is by no means smooth. The float motion, however, is an indicator of where the water from 1000 m depth would go, were the chimney to collapse. It would clearly move around the north of the Greenland Sea gyre, then enter the East Greenland Current and, presumably, pass over the Denmark Strait overflow to join the North Atlantic Deep Water. The latest evidence from the drift of the 75˚/0˚chimney suggests that it has become released from whatever force was keeping it near a fixed location, and is now moving in the same general direction as this intermediate water.

The effect of chimneys on the surrounding water mass

The absence of deep convection over the past three decades has led to a slow but steady warming of Greenland Sea Deep Water temperature (Visbeck & Rhein 2000). There is the additional phenomenon of the deep, and steadily deepening, temperature maximum discussed by Budéus et al. (1998). The potential temperature below 2500 m has increased from just below –1.3˚C in 1970 to –1.11˚C in 2002. Do chimneys play a role in this warming?

Figure 15B gives an example of how a chimney influences the water column well below its convection depth. This is also shown in Figure 29 (see colour insert) where the depth of this deep temperature maximum has been plotted, showing how it is depressed below the chimney. Figure 30A (see colour insert) shows a temperature slice from S01 at the 3000-dbar level, showing that the temperature at this depth is about –1.07˚C in the region surrounding the chimney, whereas directly below the chimney centre the temperature is –1.00˚C. Even at a depth of 3500 m the background temperature is –1.11˚C, and directly under the chimney it has risen to –1.09˚C. Our conclusion is that in "pushing down" the temperature maximum layer rather than penetrating it, the chimney is also pushing down the Greenland Sea Deep Water beneath the temperature maximum, causing some outward flow along the bottom and enhancing the bottom water temperature. Chimneys therefore can be a cause of a local increase of bottom water temperature, as well as of salinity, as can be seen from an analogous argument using the salinity slice of Figure 30B. This increase is not only local but also, presumably, temporary, for when the chimney moves away, its influence on the underlying water moves with it. It could be used, for instance, as a way of detecting chimneys by mounting a sensitive temperature sensor on the seabed. The downward displacement of water from T_{max} below the chimney constitutes the equivalent of a single act of convection, in that the water within a volume approximately that of a cylinder 20 km in diameter and 1000 m thick (~300 km^3) is being moved downward by about 1000 m.

The influence of the chimney on the water that surrounds it laterally can be considered in terms of the range of influence and water composition in the so-called outer zone of the chimney. The inner core of the chimney is a column, with uniform water properties, extending down to 2500 m and pushing down the water at the temperature maximum and below to greater depths. The outer zone rotates more slowly, has intermediate water properties, and is uniform down to lesser depths. What is its origin?

For winter 2001, Table 1 shows results from mixing of water from station 10, the core of the chimney, with various proportions of water from station 13 about 17 km from the centre of the chimney, and thus outside the chimney region and representative of the background water properties. The binary combinations were compared to station 11, approximately 5 km from the central chimney station and within the outer zone. Assuming that mixing takes place within and not across isopycnals, then the background water, which is able to mix with the water from the core of the chimney (± 0.005 kg m^{-3}), is to be found between 980 and 1175 dbar and has a potential temperature ranging from – 0.940 to – 0.956˚C (mean of – 0.949˚C) and a salinity of 34.875 to 34.877 (mean

Table 1 Proportions of binary mixes at different depths that give properties coinciding with those of the chimney skirt

Pressure (dbar)		Chimney core (Stn 10) (P1)	Background water (Stn 13) (P2)	Mixture % P1 + % P2	Predicted skirt	Chimney skirt (Stn 11)
0–500	Salinity	34.880	34.884	43.5, 56.5	34.882	34.882
	Potential temperature	–1.042	–0.950		–0.990	–0.990
500–1000	Salinity	34.880	34.884	62.0, 38.0	34.881	34.881
	Potential temperature	–1.042	–0.950		–1.007	–1.007
1000–1500	Salinity	34.880	34.884	72.8, 27.2	34.881	34.881
	Potential temperature	–1.042	–0.950		–1.017	–1.017
1500–2000	Salinity	34.880	34.884	84.8, 15.2	34.881	34.881
	Potential temperature	–1.042	–0.950		–1.029	–1.028

Note: Stn = station.

of 37.876). As the potential temperature and salinity of the skirt vary with depth, we have broken the mixing into 500-dbar ranges.

The match with both salinity and temperature demonstrates that water mass modification can occur through the entrainment of background water within the chimney skirt or outer zone, with the shallower parts entraining more surrounding water than the deeper parts. This suggests that the outer zone or skirt of the chimney is the place where interaction with surrounding water occurs, and that it is here that water may be flowing into the chimney system, to be expelled at greater depth after mixing and convecting.

During the period between W01 and S01 the waters within the skirt region were further modified, but of particular interest is that water mass modification has occurred within the central core region of the chimney. The period between W01 and S01 generally corresponds to a negative ocean–atmosphere heat flux, i.e., heat gained by the ocean, and thus the chimney will be in a nonconvective state with respect to atmospheric forcing. Furthermore, the chimney is capped with a lens of warm, relatively less saline water, and thus the modification probably occurred laterally, i.e., through the sides of the chimney. As with W01 skirt water, the modification is not homogeneous with depth but shows an increased modification in the upper regions of the chimney.

Binary calculations of the amount of mixing between background water and the core were performed using the same technique as above except that the value of the original chimney water in S01 was taken as between 2000 and 2200 dbar. The upper 150 dbar was not included in the calculation, as this water mass was influenced by the capping process. Station 39 was the centre of the core while station 42 was taken as the background. Results can be seen in Table 2.

Table 2 shows that some entrainment of background water into the central region of the chimney has occurred, but only above the 1500-dbar level. From both W01 and S01 a picture emerges of a chimney that is susceptible to the slow entrainment of the background water mass from the sides. This entrainment occurs preferentially in both the upper and outer sections of the chimney. There is no reason why the process will not continue during the lifetime of the chimney, and thus the water within the chimney will slowly evolve. The cap of the chimney complicates this picture, since in winter the cap is convected downward, thus modifying the chimney further. However, if the skirt becomes more saline due to entrainment, one can envisage the entrainment process increasing the salinity and thus density of the skirt area before the central region.

Table 2 Binary mixes at freshwater depths that give properties corresponding to the chimney core

Pressure (dbar)		Chimney core (2000–2200 dbar) (P1)	Background water (P2)	Mixture % P1 + % P2	Chimney core	Predicted core
150–500	Salinity	34.880	34.885	63.5, 36.5	34.882	34.882
	Potential temperature	–1.041	–0.934		–1.002	–1.002
500–1000	Salinity	34.880	34.885	83.2, 16.8	34.881	34.881
	Potential temperature	–1.041	–0.934		–1.023	–1.023
1000–1500	Salinity	34.880	34.885	95.3, 4.7	34.880	34.880
	Potential temperature	–1.041	–0.934		–1.036	–1.036
1500–2000	Salinity	34.880	34.885	100, 0	34.880	34.880
	Potential temperature	–1.041	–0.934		–1.041	–1.041

Possible mechanisms of chimney generation

The results of the winter 2003 fieldwork suggest that chimney formation is difficult in the Greenland Sea but that it is not unique to one location. This result raises the question of the origin of the chimneys. Figure 11 shows the position of the W01 chimney relative to the Greenland Sea Fracture Zone. It was speculated that some intermediate water from the East Greenland Current may be diverted to the SE along the far face of the fracture zone, and that when it passes through gaps in the zone to spread into the central part of the gyre, it loses geostrophic balance, causing instabilities that may result in eddy formation. The eddies then meet downward-reaching convective plumes in winter, amalgamating to create a chimney. To test this hypothesis, three stations were carried out in May 2003 along the flank of the Greenland Sea Fracture Zone and one in the centre of the gap that was closest to the chimney (Figure 22). In no case was a candidate water mass detected. In fact, the profiles resembled closely the conventional T,S profiles found inside the grid area.

An alternative hypothesis harks back to salt flux theory. During most winters until 1997 the central gyre region was covered by the locally formed regime of frazil–pancake ice known as the Odden (Comiso et al. 2001). This yielded a salt flux that was an effective way of increasing surface density. Salt flux models (p. 7), which consider both ice growth and advection, predict that in an Odden year the sea surface in the vicinity of 75˚/0˚ does indeed acquire sufficiently increased density for overturning during winter. However, the Odden ice tongue has not reached the gyre centre since 1997, possibly due to the prevalence of a phase of the Arctic oscillation, which leads to warm easterly winds over the region in preference to cold NW wind outbreaks. If each of the rotating floats used by Gascard et al. (2002) is identified with a separate chimney, his data suggest a population of several chimneys present in the area in 1997. Models of chimneys (Killworth 1979, 1983) suggest that a population of 6–12 chimneys forming and dissipating within a single year would produce enough ventilation to account for observed changes in the Greenland Sea Deep Water. If we adopt the hypothesis that ice formation is necessary for chimney formation, then in 1997 several chimneys may have formed that have since dissipated or moved away without further reinforcement, so that by 2003 only two chimneys survive. It is already known that a chimney can survive at least 26 months, implying a long-term stability that may be maintained by the surface forcing during winter, so a survival time of 6 yr is not impossible. In this respect the chimney resembles the submesoscale coherent vortices (SCVs) found at mid-depths in the Mediterranean outflow (Armi et al. 1989), which can also be long-lived.

Conclusions and prospects

The author's view is that despite the mass of new evidence now available from this chimney, we still do not have enough information to be able to specify a mechanism for its formation. It is possible, for instance, that it is very long-lived: it appears to be able to renew itself from year to year, being capped in summer but getting rid of the cap in early winter and reestablishing a homogeneous rotating column. Until we learn how this is done (including how angular momentum is retained or regained), we cannot specify how old the chimney is. Therefore, we cannot rule out freezing and salt rejection as a formation mechanism, unlikely as it may seem given that the last locally formed ice in the shape of the Odden ice tongue covered this region in 1997.

The present state of our knowledge can be summarised thus:

1. A remarkably stable, anticyclonically rotating (with angular velocity of f/2), convective chimney has been observed in the Greenland Sea at 75°N 0°W, with uniform water properties to a depth of 2500 m. It has survived 26 months from the first to the most recent observation.
2. The chimney was first observed in winter 2001, persisted through summer 2001, while being capped by a 50-m surface layer of warm low-salinity water and further intrusions of higher-salinity water down to 500 m, and was observed as open again to the surface in winter 2002. It was observed again in summer 2002 in a capped condition, and again in April and May 2003 with apparently partial capping. The near-surface structure suggests that it did not reopen completely to the surface during the 2002–3 winter.
3. The chimney is surrounded by a water mass that has a temperature maximum at 1500–1800 m depth, but beneath the chimney this same maximum occurs at about 2800 m, giving the impression that the maximum and the water below it have been pushed down. This also causes the seabed temperature to be raised under the chimney, giving a "warm shadow" of the chimney on the seabed.
4. The inner structure of the chimney is of a core 10 km in diameter in solid body rotation and an outer zone or skirt of 20 km diameter, rotating more slowly. Binary analysis suggests that the skirt is composed of a mixture of water from the core and water from the surroundings, with the proportion of water from outside being greatest at shallow depths. In summer some entrainment also happens into the core waters at depths of less than 1500 m.
5. A second chimney has been discovered in the Greenland Sea in May 2003, also in the eastern part of the central gyre region and 70 km from the first chimney.
6. The two chimneys differ in core parameters, the second being warmer than the first, indicating a different time, place, or mode of formation.
7. There are currently no other chimneys within an area of 15,000 km^2 covering the central part of the gyre, which is most susceptible to overturning. It is concluded that the number of chimneys existing in the gyre at the time of our survey was either two or a number only slightly greater (three or four). This is much less than the probable population of chimneys in 1997, the last year of a locally formed ice cover.
8. The 75°/0°chimney began by being confined within a very small region, but during 2003 it has become much more mobile. It is now advecting along approximately the trajectory of intermediate water and may be on its way out of the gyre centre.

These new results emphasise the importance of the variable role of chimneys in Greenland Sea dynamics and thus in rapid climate change. Models suggest that if indeed the volume of convection in the Greenland Sea is seriously declining, then there will be an adverse impact on NW European climate after a few decades (Rahmstorf & Ganopolski 1999). It is therefore important to continue to monitor these fascinating structures, especially in winter.

Acknowledgements

The author is grateful to the Norsk Polarinstitutt, Tromsø, for supporting the 2003 cruise of LANCE; to Alfred-Wegener-Institut for support for POLARSTERN in 2003; and to the European Community for support of the ESOP-1, ESOP-2, and CONVECTION projects and their associated cruises. The present paper was an output from the CONVECTION project of the Environment and Sustainable Development programme, contract EVK2-CT-2000-00058.

References

Aagaard, K. & Carmack, E.C. 1989. The role of sea ice and other fresh water in the Arctic circulation. *Journal of Geophysical Research* **94** (C10), 14485–14498.

Aagaard, K., Swift, J.H. & Carmack, E.C. 1985. Thermohaline circulation in the Arctic Mediterranean seas. *Journal of Geophysical Research* **90** (C3), 4833–4846.

Alekseev, G.V., Ivanov, V.V. & Korablev, A.A. 1994. Interannual variability of the thermohaline structure in the convective gyre of the Greenland Sea. In *The Polar Oceans and Their Role in Shaping the Global Environment*, O.M. Johannessen et al. (eds). American Geophysical Union, Geophysical Monograph **85**, 485–496.

Anderson, L.G., Chierici, M., Fogelqvist, E. & Johannessen, T. 2000. Flux of anthropogenic and steady-state carbon into the deep Greenland Sea. *Journal of Geophysical Research* **105**, 14339–14345.

Armi, L., Hebert, D., Oakey, N., Price, J.F., Richardson, P.L., Rossby, H.T. & Ruddik, B. 1989. Two years in the life of a Mediterranean salt lens. *Journal of Physical Oceanography* **19**, 354–370.

Backhaus, J.O. & Kämpf, J. 1999. Simulations of sub-mesoscale oceanic convection and ice-ocean interactions in the Greenland Sea. *Deep-Sea Research II* **46**, 1427–1455.

Bönisch, G., Blindheim, J., Bullister, J.L., Schlosser, P. & Wallace, D.W.R. 1997. Long term trends of temperature, salinity, density and transient tracers in the Greenland Sea. *Journal of Geophysical Research* **102**, 18553–18571.

Børsheim, K.Y. & Myklestad, S.M. 1997. Dynamics of DOC in the Norwegian Sea inferred from monthly profiles collected during three years at 66°N, 2°E. *Deep-Sea Research* **44**, 593–601.

Brewer, P.G., Takahashi, T. & Williams, R.T. 1986. Transient Tracers in the Ocean (TTO): Hydrographic Data and Carbon Dioxide Systems with Revised Carbon Chemistry Data. Carbon Dioxide Information Analysis Center, U.S. DOE Global Survey of CO_2 in the Oceans. http://cdiac.esd.ornl.gov/oceans/ndp004.html.

Budéus, G. 1999. European Subpolar Ocean Programme-2 (ESOP) data CD. Copenhagen, Denmark: ICES.

Budéus, G., Cisewski, B., Ronski, S., Dietrich, D. & Weitere, M. 2004. Structure and effects of a long lived vortex in the Greenland Sea. *Geophysical Research Letters*, **31**, L05304, doi:10.1029/2003 GL017983.

Budéus, G., Schneider, W. & Krause, G. 1998. Winter convective events and bottom water warming in the Greenland Sea. *Journal of Geophysical Research* **103** (C9), 18513–18527.

Carmack, E.C. & Aagaard, K. 1973. On the deep water of the Greenland Sea. *Deep-Sea Research* **20**, 687–715.

Chen, C.-T.A., Jones, E.P. & Lin, K. 1990. Wintertime total carbon dioxide measurements in the Norwegian and Greenland Seas. *Deep-Sea Research* **37**, 1455–1473.

Clarke, R.A. & Gascard, J.-C. 1983. The formation of Labrador Sea Water. Part I. Large-scale processes. *Journal of Physical Oceanography* **13**, 1764–1778.

Clarke, R.A., Swift J.H., Reid, J.L. & Koltermann, K.P. 1990. The formation of Greenland Sea Deep Water: double diffusion or deep convection? *Deep-Sea Research* **37**, 1385–1424.

Comiso, J.C., Wadhams, P., Pedersen, L.T. & Gersten, R.A. 2001. Seasonal and interannual variability of the Odden ice tongue and a study of environmental effects. *Journal of Geophysical Research* **106** (C5), 9093–9116.

Fischer, K.W., Legg, S., Munk, W.H., Shuchman, R.A., Garwood, R.W. & Palshook, J.P. 1999. Modeled radar surface signature of deep ocean convection. *IEEE Transactions of Geoscience and Remote Sensing* **37**, 2050–2067.

Foldvik, A., Aagaard, K. & Tørresen, T. 1988. On the velocity field of the East Greenland Current. *Deep-Sea Research* **35**, 1335–1354.

Galbraith, P.S. & Kelley, D.E. 1996. Identifying overturns in CTD profiles. *Journal of Atmospheric and Oceanic Technology* **13**, 688–702.

Garwood, R.W., Jr., Isakari, S.M. & Gallacher, P.C. 1994. Thermobaric convection. In *The Polar Oceans and Their Role in Shaping the Global Environment*, O.M. Johannessen et al. (eds). American Geophysical Union, Geophysical Monograph **85**, 199–209.

Gascard, J.-C. 1999. The floats release experiment. In *The Thermohaline Circulation in the Greenland Sea: Final Scientific Report*, E. Jansen & V. Opheim (eds). European Union contract MAS3-CT95-0015, Brussels.

Gascard, J.-C. & Clarke, R.A. 1983. The formation of Labrador Sea Water. Part II. Mesoscale and smaller-scale processes. *Journal of Physical Oceanography* **13**, 1779–1797.

Gascard, J.-C., Richez, C. & Rouault, C. 1995. New insights on large scale oceanography of Fram Strait: the West Spitsbergen Current. In *Arctic Oceanography: Marginal Ice Zone and Continental Shelves*, W.O. Smith & J.M. Grebmeier (eds). Coastal and Estuarine Studies **49**, 131–182, AGU, Washington.

Gascard, J.-C., Watson, A.J., Messias, M.-J., Olsson, K.A., Johannessen, T. & Simonsen, K. 2002. Long-lived vortices as a mode of deep ventilation in the Greenland Sea. *Nature* **416**, 525–527.

Gill, A.E. 1981. Homogeneous intrusions in a rotating stratified fluid. *Journal of Fluid Mechanics* **103**, 275–295.

Gradinger, R., Friedrich, C. & Spindler, M. 1999. Abundance, biomass and composition of the sea ice biota of the Greenland Sea pack ice. *Deep-Sea Research II* **46**, 1457–1472.

GSP Group. 1990. Greenland Sea Project. A venture toward improved understanding of the oceans' role in climate. *EOS, Transactions of the American Geophysical Union* **71**, 750–755.

Häkkinen, S. 1987. A coupled dynamic-thermodynamic model of an ice-ocean system in the marginal ice zone. *Journal of Geophysical Research* **92**, 9469–9478.

Hedstrom, K. & Armi, I. 1988. An experimental study of homogeneous lenses in a stratified rotating fluid. *Journal of Fluid Mechanics* **191**, 535–556.

Helland-Hansen, B. & Nansen, F. 1909. *The Norwegian Sea: Its Physical Oceanography Based on the Norwegian Researches 1900–1904. Report on Norwegian Fishery and Marine Investigations*. Christiania **2**, 390 pp.

Honjo, S., Manganini, S.J., Karowe, A. & Woodward, B.L. 1987. Particle Fluxes, North-Eastern Nordic Seas: 1983–1986, Technical Report WHOI-87-17. Woods Hole Oceanographic Institution.

Hood, E.M., Merlivat, L. & Johannessen, T. 1999. fCO_2 variations and air sea flux of CO_2 in the Greenland Sea gyre using high-frequency time series from CARIOCA drift buoys. *Journal of Geophysical Research* **104** (C9), 20571–20583.

Killworth, P.D. 1979. On chimney formation in the ocean. *Journal of Physical Oceanography* **9**, 531–554.

Killworth, P.D. 1983. Deep convection in the world ocean. *Reviews of Geophysics* **21**, 1–26.

Lab Sea Group. 1998. The Labrador Sea Deep Convection Experiment. *Bulletin of the American Meteorological Society* **79**, 2033–2058.

Lherminier, P., Harcourt, R.R., Garwood, R.W., Jr. & Gascard, J.-C. 2001. Interpretation of mean vertical velocities measured by isobaric floats during deep convection events. *Journal of Marine Systems* **29**, 221–237.

Marshall, J. & Schott, F. 1999. Open-ocean convection: observations, theory and models. *Reviews of Geophysics* **37**, 1–64.

Mauritzen, C. 1996a. Production of dense overflow waters feeding the North Atlantic across the Greenland–Scotland Ridge. Part 1. Evidence for a revised circulation scheme. *Deep-Sea Research* **43**, 769–806.

Mauritzen, C. 1996b. Production of dense overflow waters feeding the North Atlantic across the Greenland–Scotland Ridge. Part 2. An inverse model. *Deep-Sea Research* **43**, 807–835.

McDougall, T.J. 1983. Greenland Sea bottom water formation: a balance between advection and double-diffusion. *Deep-Sea Research* **30**, 1109–1117.

Medoc Group. 1970. Observation of formation of deep water in the Mediterranean Sea. *Nature* **227**, 1037–1041.

Miller, L.A., Chierici, M., Johannessen, T., Noji, T.T., Rey, F. & Skjelvan, I. 1999. Seasonal dissolved inorganic carbon variations in the Greenland Sea and implications for atmospheric CO_2 exchange. *Deep-Sea Research II* **46**, 1473–1496.

Morawitz, W.M.L., Sutton, P.J., Worcester, P.F., Cornuelle, B.D., Lynch J.F. & Pawlowicz, R. 1996. Three-dimensional observations of a deep convective chimney in the Greenland Sea during winter 1988/89. *Journal of Physical Oceanography* **26**, 2316–2343.

Mosby, H. 1959. Deep water in the Norwegian Sea. *Geofysiks Publications* (University of Bergen) **21**, 62 pp.

Nansen, F. 1906. Northern waters. Captain Roald Amundsen's oceanographic observations in the Arctic Seas in 1901. *Videnskabelige Selsk. Skr. I. Mathematisk-Natur. Klasse*. Christiania, J. Dybwad, 145 pp.

Noji, T.T., Rey, F., Miller, L.A., Børsheim, K.Y. & Urban-Rich, J. 1999. Fate of biogenic carbon in the upper 200 m of the central Greenland Sea. *Deep-Sea Research II* **46**, 1497–1510.

Pickart, R.S., Spall, M.A., Ribergaard, M.H., Moore, G.W.K. & Milliffs, R.F. 2003. Deep convection in the Irminger Sea forced by the Greenland tip jet. *Nature* **424**, 152–156.

Quadfasel, D., Gascard, J.-C. & Koltermann, K.P. 1987. Large scale oceanography in Fram Strait during the 1984 Marginal Ice Zone Experiment. *Journal of Geophysical Research* **92** (C7), 6719–6728.

Rahmstorf, S. & Ganopolski, A. 1999. Long-term global warming scenarios computed with an efficient coupled climate model. *Climatic Change* **43**, 353–367.

Rhein, M. 1991. Ventilation rates of the Greenland and Norwegian Seas derived from distributions of the chlorofluoromethanes F11 and F12. *Deep-Sea Research* **38**, 485–503.

Rhein, M. 1996. Convection in the Greenland Sea, 1982–1993. *Journal of Geophysical Research* **101** (C8), 18183–18192.

Roach, A.T., Aagaard, K. & Carsey, F.D. 1993. Observations of vertical currents and convection in the central Greenland Sea during the winter of 1988–1989. *Journal of Geophysical Research* **98** (C11), 203–235.

Rudels, B. 1990. Haline convection in the Greenland Sea. *Deep-Sea Research* **37**, 1491–1511.

Rudels, B., Friedrich, H.J. & Quadfasel, D. 1999. The Arctic Circumpolar Boundary Current. *Deep-Sea Research II* **46**, 1023–1062.

Rudels, B. & Quadfasel, D. 1991. Convection and deep water formation in the Arctic Ocean: Greenland Sea system. *Journal of Marine Systems* **2**, 435–450.

Rudels, B., Quadfasel, D., Friedrich, H. & Houssais, M.-N. 1989. Greenland Sea convection in the winter of 1987–1988. *Journal of Geophysical Research* **94**, 3223.

Sandven, S., Johannessen, O.M. & Johannessen, J.A. 1991. Mesoscale eddies and chimneys in the marginal ice zone. *Journal of Marine Systems* **2**, 195–208.

Schlichtholtz, P. & Houssais, M.-N. 1999a. An inverse modelling study in Fram Strait. Part I. Dynamics and circulation. *Deep-Sea Research II* **46**, 1083–1136.

Schlichtholtz, P. & Houssais, M.-N. 1999b. An inverse modelling study in Fram Strait. Part II. Water mass distribution and transports. *Deep-Sea Research II* **46**, 1137–1168.

Schlosser, P., Bönisch, G., Rhein, M. & Bayer, R. 1991. Reduction of deepwater formation in the Greenland Sea during the 1980s: evidence from tracer data. *Science* **251**, 1054–1056.

Schott, F.M., Visbeck, M. & Fischer, J. 1993. Observations of vertical currents and convection in the central Greenland Sea during the winter of 1988/9. *Journal of Geophysical Research* **98** (C8), 14401–14421.

Scoresby, W., Jr. 1815. On the Greenland or Polar Ice. *Memoirs of the Wernerian Society* **2**, 328–336. (Reprinted 1980, Caedmon of Whitby Press, Whitby.

Scoresby, W., Jr. 1820. *An Account of the Arctic Regions, with a History and Description of the Northern Whale-Fishery.* Edinburgh: Constable. (Reprinted 1969, Newton Abbot: David & Charles.)

Shuchman, R.A., Josberger, E.G., Russel, C.A., Fischer, K.W., Johannessen, O.M., Johannessen, J. & Gloersen, P. 1998. Greenland Sea Odden sea ice feature: intra-annual and interannual variability. *Journal of Geophysical Research* **103** (C6), 12709–12724.

Skjelvan, I., Johannessen, T. & Miller, L.A. 1999. Interannual variability of fCO_2 in the Greenland and Norwegian Seas. *Tellus B* **51**, 477–489.

Slagstad, D., Downing, K., Carlotti, F. & Hirche, H.-J. 1999. Modelling the carbon export and air–sea flux of CO_2 in the Greenland Sea. *Deep-Sea Research II* **46**, 1511–1530.

Thorkildsen, F. & Haugan, P.M. 1999. Modelling of deep-water renewal through cold convective plumes. *Deep-Sea Research II* **46**, 1357–1383.

Toudal, L. 1999. Ice extent in the Greenland Sea 1978–1995. *Deep-Sea Research II* **46**, 1237–1254.

Toudal, L. & Coon, M.D. 2001. Interannual variability of the sea-ice-induced salt flux in the Greenland Sea. *Annals of Glaciology* **33**, 385–390.

Uscinski, B.J., Kaletzky, A., Stanek, C.J. & Rouseff, D. 2003. An acoustic shadowgraph trial to detect convection in the Arctic. *Waves in Random Media* **13**, 107–123.

Vinje, T.E. 1977. Sea ice conditions in the European sector of the marginal seas of the Arctic, 1966–75. *Norsk Polarinstitutt Årbok 1975*, 163–174.

Visbeck, M., Fischer, J. & Schott, F. 1995. Preconditioning the Greenland Sea for deep convection: ice formation and ice drift. *Journal of Geophysical Research* **100** (C9), 18489–18502.

Visbeck, M. & Rhein, M. 2000. Is bottom boundary layer mixing slowly ventilating Greenland Sea Deep Water? *Journal of Physical Oceanography* **30**, 215–224

Wadhams, P. 1999. The Odden ice tongue and Greenland Sea convection. *Weather* **54** (3), 83–84, 91–97.

Wadhams, P., Comiso, J.C., Prussen, E., Wells, S., Brandon M., Aldworth, E., Viehoff, T., Allegrino, R. & Crane, D.R. 1996. The development of the Odden ice tongue in the Greenland Sea during winter 1993 from remote sensing and field observations. *Journal of Geophysical Research* **101** (C8), 18213–18235.

Wadhams, P., Holfort, J., Hansen, E. & Wilkinson, J.P. 2002. A deep convective chimney in the winter Greenland Sea. *Geophysical Research Letters* **29**, doi: 10.1029/2001 GL014306.

Wadhams, P., Miller, L. & Gascard, J.-C. 1999. The European Subpolar Ocean Programme: an introduction. *Deep-Sea Research II* **46**, 1011–1022.

Wadhams, P. & Wilkinson, J. 1999. The physical properties of sea ice in the Odden ice tongue. *Deep-Sea Research II* **46**, 1275–1300.

Wadhams, P., Wilkinson, J.P., Pavlov, V., Hansen, E. & Quadfasel, D. 2004a. Long-term persistence and evolution of a deep convective chimney in the Greenland Sea. *Journal of Physical Oceanography*, **31**, L06306, doi:10.1029/2003 GL019017.

Wadhams, P., Budéus, G., Wilkinson, J.P., Løyning, T. & Pavlov, V. 2004b. The multi-year development of long-lived convective chimneys in the Greenland Sea. *Geophysical Research Letters*, in press.

Watson, A.J., Messias, M.J., Fogelqvist, E., Van Scoy, K.A., Johannessen, T., Oliver, K.I.C., Stevens, D.P., Rey, F., Tanhua, T., Olsson, K.A., Carse, F., Simonsen, K., Ledwell, J.R., Jansen, E., Cooper, D.J., Kruepke, J.A. & Guilyardi, E. 1999. Mixing and convection in the Greenland Sea from a tracer-release experiment. *Nature* **401**, 902–904.

Wilkinson, J.P. & Wadhams, P. 2003. A salt flux model for salinity change through ice production in the Greenland Sea, and its relationship to winter convection. *Journal of Geophysical Research* **108** (C5), 3147, doi: 10.1029/2001 JC001099.

Wilkinson, J.P., Wadhams, P. & Toudal, L. 1999. Ice motion field over the Odden area. In *The Thermohaline Circulation in the Greenland Sea: Final Scientific Report*, E. Jansen & V. Opheim (eds). European Union contract MAS3-CT95-0015, Brussels.

Wood, R.A., Keen, A.B., Mitchell, J.F.B. & Gregory, J.M. 1999. Changing spatial structure of the thermohaline circulation in response to atmospheric CO_2 forcing in a climate model. *Nature* **399**, 572–575.

THE ROLE OF DIMETHYLSULPHOXIDE IN THE MARINE BIOGEOCHEMICAL CYCLE OF DIMETHYLSULPHIDE

ANGELA D. HATTON,[1]* LOUISE DARROCH[2] & GILL MALIN[2]
[1]*Scottish Association for Marine Science, Dunstaffnage Marine Laboratory, Oban, Argyll, PA37 1QA, U.K.*
[2]*School of Environmental Sciences, University of East Anglia, Norwich, NR4 7TJ, U.K.*
*E-mail: Angela.Hatton@sams.ac.uk

Abstract Dimethylsulphoxide ($(CH_3)_2SO$; DMSO) occurs naturally in marine and freshwater environments, rainwater, and the atmosphere. It is thought to be an environmentally significant compound due to the potential role it plays in the biogeochemical cycle of the climatically active trace gas, dimethylsulphide (DMS). Generally it has been assumed that the photochemical and bacterial oxidations of DMS to DMSO represent major sources of this compound and significant sinks for DMS in the marine environment. Conversely, it has also been suggested that DMSO may be a potential source for oceanic DMS. Recent research has improved understanding of the origin and fate of DMSO in sea water, although it seems likely that the full role this compound may play in the marine sulphur cycle has still to be elucidated. The methods available for determining DMSO in aqueous samples and current knowledge of the distribution of DMSO in marine waters are reviewed. Mechanisms for DMSO production and loss pathways are also considered, as well as the possible role this compound may play in the cycling of DMS and global climate.

Introduction

Dimethylsulphoxide (DMSO), the simplest of the homologous series of organic sulphoxides, is well known for its unique solvent properties (David 1972) and is produced either as a waste product of the papermaking industry or commercially by oxidation of dimethylsulphide (DMS) with dinitrogen tetroxide (Robbins 1961). It is a colourless, strongly hygroscopic, nonvolatile liquid that has a boiling point at 189°C and a melting point at 18.45°C. Among its many applications, DMSO is widely used in cell biology and is well known as a cryoprotectant for the preservation of living cells and tissues (Yu & Quinn 1994). DMSO has also been widely used for diverse medical applications. Pharmaceutical interest is mainly due to its analgesic and anti-inflammatory properties (Evans et al. 1993, Shimoda et al. 1996) and its ability to deliver drugs through the skin (Anigbogu et al. 1995). There is also some evidence that DMSO may reduce the development of cancer because of its free-radical scavenging properties (Bertelli et al. 1993, Diamond et al. 1997), and it has been suggested that DMSO has an antibacterial action, may act as a sedative (David 1972) and can both reduce the infectivity of HIV *in vitro* and bring about the systematic improvement in advanced AIDS patients (Aranda-Anzaldo et al. 1992).

DMSO occurs naturally in a wide range of beverages and foodstuffs, including fruits, vegetables, wine, and beer (Pearson et al. 1981, de Mora et al. 1993, Yang & Schwarz 1998). In addition, it has been detected in freshwater lakes and streams (Andreae 1980a, Richards et al. 1994), Antarctic

0-8493-2727-X/04/$0.00+$1.50
Oceanography and Marine Biology: An Annual Review 2004 **42**, 29–56

glacial meltwater ponds (de Mora et al. 1996), Arctic coastal sea ice (Lee et al. 2001), sea water (Gibson et al. 1990, Kiene & Gerard 1994, Simó et al. 1995, 1997, 1998b, 2000, Lee & de Mora 1996, Hatton et al. 1996, 1998, 1999, Lee et al. 1999a, Bouillon et al. 2002), rainwater (Harvey & Lang 1986, Ridgeway et al. 1992, Hatton 1995, Lee et al. 2001) and the atmosphere (Berresheim et al. 1993, Sciare & Mihalopoulos 2000).

In marine biogeochemistry, interest in the distribution of DMSO focuses around the idea that DMSO could be a key compound in the marine biogeochemical cycle of DMS, which is considered to be one of the most important biogenic sulphur compounds in the marine environment. It has been suggested that DMS could be both chemically and biologically oxidised within the marine environment, leading to the formation of DMSO, and as such, DMSO is expected to play an important role in DMS biogeochemistry. However, until recently the few available measurements for DMSO in sea water were thought to be unreliable due to analytical difficulties (Hatton et al. 1994b). The development of a new sensitive technique (Hatton et al. 1994b) and the refinement of previously established methods (Kiene & Gerard 1994, Simó et al. 1996, 1998b) have now shown that DMSO is present in sea water at concentrations equal to or higher than DMS (Hatton et al. 1996, 1999, Simó et al. 2000). Additional progress has been made regarding the origin and fate of this compound, although its role in the marine sulphur cycle has still to be fully established. In this paper the global importance of DMS, its marine biogenic origin and the potential role DMSO may play in the biogeochemical cycle of this important trace gas are briefly discussed.

The global significance of DMS

All models for the biogeochemical cycle of sulphur require volatile or gaseous compounds to provide a vehicle for the transfer of sulphur from the sea to land surfaces. In past considerations of the marine sulphur cycle it was the inorganic sulphur compounds that received the most attention. Consequently, the oxidation–reduction circuit between sulphate and sulphide, with hydrogen sulphide as the gaseous link, was for a long time considered to explain most of the biologically driven flow of sulphur in the natural environment (Kelly & Baker 1990). In 1972, however, Lovelock et al. published evidence for the ubiquity of DMS in surface sea water and proposed that marine DMS was the natural sulphur compound filling the role originally assigned to H_2S. At that time it was already known that many living systems, including marine algae, produced DMS, and biochemical data were available that suggested that dimethylsulphoniopropionate (DMSP) might be the precursor of DMS in marine ecosystems (Challenger 1951, Cantoni & Anderson 1956, Tocher & Ackman 1966, Ishida 1968, Kadota & Ishida 1968). It is now well established that DMS is the major volatile sulphur species in the oceans and this fact, along with the suggestion that DMS may play an important role in climate and atmospheric chemistry (Charlson et al. 1987, Andreae 1990, Bates et al. 1992), has led to a great deal of research focusing on this compound. Since the early 1980s, DMS measurements have been made throughout the Pacific, Atlantic, Arctic, Indian, and Southern Oceans (see Kettle et al. 1999 and references therein). These studies have shown that DMS is normally restricted to the upper 200 m of the water column, with higher concentrations found on continental shelves and in high productivity regions.

Relative to concentrations of DMS in the atmosphere, the surface oceans have been shown to be typically two orders of magnitude supersaturated, implying a net flux of the gas from the oceans to the atmosphere (Liss & Slater 1974, Andreae 1986, Liss et al. 1993). In the atmosphere, the rapid oxidation of DMS leads to the production of sulphur dioxide (SO_2), sulphate, and methane sulfonate (MSA), with sulphate and MSA present in the atmosphere predominantly in the form of aerosol particles. These aerosols may be deposited in rain and snow, thereby contributing to the acidity of natural precipitation (Plane 1989), and may act as cloud condensation nuclei (CCN) over the remote oceans (Charlson et al. 1987). During the 1980s concern over acid rain increased interest in the relative strengths of the various sources of sulphur to the atmosphere (Bates & Cline 1985). Due to this concern, many studies were conducted to calculate the sea–air fluxes of DMS and other sulphur gases, such as carbonyl sulphide, carbon disulphide, and dimethyl disulphide (e.g., Barnard et al. 1982, Andreae & Raemdonck 1983, Andreae et al. 1983, 1994, Andreae & Barnard 1984, Bates et al. 1987, Erickson et al. 1990, Malin et al. 1993).

Fluxes are generally calculated from field measurements of DMS in sea water and estimates of the transfer velocity, the term that quantifies the rate of transfer. Gases are transferred across the air–sea interface by a combination of molecular and turbulent diffusion processes, which are influenced by wind speed, boundary layer stability, surfactants, and bubbles (Liss & Merlivat 1986, Wanninkhof 1992, Nightingale et al. 2000). Current understanding of the processes controlling the air–sea exchange of trace gases is covered in the recent monograph by Donelan et al. (2002), and specific discussions on DMS emissions can be found in Malin (1996) and Turner et al. (1996). To summarise, the sea-to-air flux of DMS is currently estimated to be of the order of 15–33 Tg of sulphur yr^{-1} (Kettle et al. 1999). This flux accounts for a large fraction of total biogenic sulphur emissions (15–50 Tg sulphur yr^{-1}, Chin & Jacob 1996), such that DMS makes a major contribution to the atmospheric sulphur pool, and hence the chemistry and radiative properties of the atmosphere (Simó 2001).

DMS and its biogenic origins in sea water

DMS is formed mainly from the enzymatic breakdown of DMSP, a compatible solute produced by marine algae to maintain their osmotic balance in sea water (Vairavamurthy et al. 1985, Dacey & Wakeham 1986). However, it has also been suggested that marine phytoplankton may produce DMSP as a cryoprotectant (Kirst et al. 1991, Lee & de Mora 1999), an antioxidant (Sunda et al. 2002), a methyl donor for a variety of biochemical processes (Cantoni & Anderson 1956, Ishida 1968, Kiene 1996), or a grazing deterrent (Wolfe et al. 1997, 2002). Furthermore, it has been hypothesised that DMSP may be produced as an overflow mechanism enabling cells to keep cysteine and methionine concentrations at a level that is low enough to prevent feedback mechanisms and allow continued sulphate assimilation even under nitrogen-limited conditions (Stefels 2000). In the early 1980s Barnard et al. (1982) and Bates & Cline (1985) noted that the distribution of DMS and DMSP only correlated in a rather general way with phytoplankton biomass, leading them to suggest that only certain groups of phytoplankton may produce significant amounts of DMSP. Subsequently, it was shown that some taxonomic groups, such as dinoflagellates and prymnesiophytes, can contain high DMSP concentrations per unit cell volume, while diatoms have variable but generally low concentrations (Keller et al. 1989).

DMS production and removal processes

The production of DMS from intracellular DMSP by healthy, growing cells was generally thought to be relatively insignificant (Turner et al. 1988, Keller et al. 1989). Experimental evidence suggests that DMSP must first be released into the surrounding sea water by zooplankton grazing (Dacey & Wakeham 1986, Leck et al. 1990, Malin et al. 1994, Wolfe et al. 1994), viral lysis (Hill et al. 1998, Malin et al. 1998), and natural senescence (Turner et al. 1988, Leck et al. 1990), where it would then be available to marine bacteria that could break down the DMSP producing DMS. Although this may be the case for many species of phytoplankton, it is now thought that some DMSP may also be cleaved within the algal cell, resulting in the direct excretion of DMS (Wolfe et al. 2002). In both cases this initial breakdown of DMSP yields DMS, acrylate, and a proton in a 1:1:1 ratio. This process is catalysed by DMSP lyase enzymes, which can be found in certain phytoplankton and bacteria (Ledyard & Dacey 1994, Stefels et al. 1996, Wolfe & Steinke 1996).

Once in sea water DMS can be removed via a number of different pathways, including ventilation to the atmosphere (Bates et al. 1987, Erickson et al. 1990), consumption by the biota (Kiene & Bates 1990, Kiene 1992, Wolfe & Kiene 1993, Ledyard & Dacey 1996), or photochemical removal (Brimblecombe & Shooter 1986, Kieber et al. 1996, Brugger et al. 1998). Current evidence suggests that the quantity of DMS emitted to the atmosphere is only a small proportion of the potential marine pool (Malin et al. 1992). Indeed, a recent estimate of the total DMS flux to the atmosphere, during a coccolithophore bloom, showed it to be equivalent to just 1.3% of the gross DMSP production and 10% of the DMS production in the surface layer (Archer et al. 2002).

Bacterial consumption of dissolved DMSP (DMSPd) and DMS is a major factor influencing the quantity of DMS available for transfer to the atmosphere. The pathways involved in DMSP degradation by aerobic microorganisms and their relative importance have been discussed in a number of reviews and so will only be briefly covered here (Taylor 1993, Taylor & Visscher 1996, Kiene et al. 2000).

Recent studies reveal that DMSP-utilising bacteria are highly active in the field (Kiene et al. 2000). It has been shown that DMSPd can undergo bacterially mediated degradation, not only via the lyase pathway to form DMS, but also via demethylation pathways yielding either 3-methiol-propionate (MMPA), which is then demethiolated producing methanethiol (MeSH), or 3-mercap-topropionate (MPA), which leads to the formation of H_2S (Taylor 1993, Kiene et al. 2000).

Several studies show that DMS is a relatively minor product of DMSPd metabolism under most circumstances in the water column (Ledyard & Dacey 1996, Van Duyl et al. 1998), and current findings favour the demethylation/demethiolation pathway as being the major fate for DMSP in sea water (Kiene et al. 2000), accounting for 75% of the DMSP bacterial transformations (Kiene & Linn 2000). Although the demethylation/demethiolation pathway is thought to be the major removal pathway for DMSP, a recent laboratory study investigated DMSP metabolism in 15 culturable bacteria of a lineage common in sea water and found that they all expressed the lyase pathway, whereas only five also expressed the demethylation pathway (Gonzàlez et al. 1999).

Following DMSPd demethylation, MeSH is incorporated into the proteins of bacterioplankton or other nonvolatile products. Studies using ^{35}S tracers showed that DMSP may be rapidly taken up into bacteria, where it remains over many hours, with a significant fraction of the tracer being shown to be assimilated into protein sulphur, primarily in the form of methionine (Kiene et al. 2000). Furthermore, it is also thought that marine bacteria may opportunistically take up DMSP to use as a compatible solute (Kiene et al. 2000). It has also been shown that marine bacteria can utilise up to 100% of the available DMS, which, in addition to being incorporated into cell biomass, has the potential for transformation to other sulphur compounds such as DMSO (Kiene & Linn 2000, Zubkov et al. 2002).

The CLAW hypothesis

In 1987 Charlson et al. put forward the CLAW hypothesis (after the initials of the authors), the controversial hypothesis that the emissions of DMS may be linked with climate regulation. The idea was that increased seawater temperature leads to increased DMS emissions, followed by atmospheric oxidation, production of CCN, and increased cloud albedo, which would serve to counteract the initial temperature increase. Thus the rate of DMS release may influence cloud formation over the oceans, which in turn affects the global heat balance, thereby giving the biota a modicum of “control” over the climate (Charlson et al. 1987). Central to this hypothesis was the assumption that DMS emissions from sea water are directly controlled by temperature. However, Malin et al. (1994) stated that because DMS emissions result from a network of production, transformation, and consumption processes, temperature could be effective at several levels. There is now little doubt that DMS is a precursor for aerosol sulphate, or that sulphate-containing aerosols are effective CCN (Schwartz 1988), and there is also persuasive theoretical evidence that these CCN may affect cloud albedo (Charlson et al. 1987, Idso 1992). Coherence between CCN con-centration and cloudiness has been documented using satellite data, strongly suggesting that DMS emissions can influence cloud radiative transfer properties (Boers et al. 1994). However, the negative feedback loop of the phytoplankton, DMS, and climate regulation hypothesis (Charlson et al. 1987) remains somewhat controversial.

Dimethylsulphoxide in sea water

Analysis of DMSO in sea water

It was always assumed that DMSO would be present in sea water and would play a role in the DMS cycle. However, this stable and soluble compound originally proved difficult to analyse at the nanomolar concentration range anticipated in marine aquatic environments. DMSO analysis is problematic because DMSO is readily soluble in water, nonionic, and cannot be purged or steam distilled (Harvey & Lang 1986). The various methods originally reported for DMSO analysis in aqueous samples were based around direct measurement, which was insufficiently sensitive for nanomolar concentration ranges (Paulin et al. 1966, Wong et al. 1971, Ogata & Fujii 1979) or chemical reduction of DMSO to DMS (Andreae 1980a), which was prone to contamination problems (Simó et al. 1998b).

Subsequently, Harvey & Lang (1986) developed a sensitive direct method for the determination of DMSO and $DMSO_2$ in rainwater and marine air masses. This method involved preconcentrating the sulphur compounds on a silica or Tenax GC column, with subsequent extraction of the compounds into methanol followed by gas chromatography. Berresheim et al. (1993) also developed a sensitive direct method for the detection of DMSO in ambient air that is based on atmospheric pressure chemical ionization/mass spectrometry (APCI/MS). However, neither of these techniques was suitable for use with saline solutions, and therefore could not be used for marine samples. One direct method for DMSO analysis has been demonstrated, which is suitable for use with seawater samples. In this case the samples were injected directly into a gas chromatograph, with increased detector sensitivity, due to the addition of sulphur hexafluoride, giving a detection limit equivalent to 0.06 nmol dm^{-3} (Lee & de Mora 1996). However, other research groups have not adopted this method.

Chemical reduction of DMSO to DMS and the subsequent analysis of DMS have greater sensitivity and are suitable for saline solutions, but most existing methods are subject to some interferences. The sample preparation technique reported by Andreae (1980b) involved the addition of sodium borohydride ($NaBH_4$) or chromium II chloride (Cr_2Cl) to bring about this reduction. However, the DMS yield by Cr_2Cl was only 42% of the expected level and the accuracy of the $NaBH_4$ method was compromised by the assumption that all DMS produced originated from DMSO, even though it had been shown that $NaBH_4$ can also initiate the conversion of DMSP to DMS and acrylic acid (Challenger & Simpson 1948, Simó et al. 1998b). Ridgeway et al. (1992) developed a novel isotope dilution method for measuring DMS and DMSO in sea water, but this method also necessitates the breakdown of DMSO with $NaBH_4$ and the use of a mass spectrometer. Chemical reduction using acidified stannous chloride to reduce DMSO to DMS has also been used, but again, this requires prior removal of DMSP by alkali hydrolysis or correction for the measured DMSP concentrations (Anness 1981, Gibson et al. 1990, Kiene & Gerard 1994).

During the past 10 yr, much work has been conducted to refine these chemical reduction methods (Kiene & Gerard 1994, Simó et al. 1996, 1998a). These refined methods along with the development of a highly specific and sensitive enzyme-linked technique (Hatton et al. 1994b) have allowed the measurement of DMSO in a variety of environments and an increased understanding of the distribution of DMSO in both fresh- and marine waters. In addition, recent suggestions that phytoplankton may produce DMSO directly (Simó et al. 1998a) have led to the development of several methods to measure nanomolar concentrations of DMSO in particulate matter (DMSOp). These methods are based on the extraction of cellular DMSO into ethanol (Lee et al. 1999a), or the disruption of cells by applying osmotic pressure or via the use of cold alkali hydrolysis (Simó et al. 1998a,b). In all cases the resulting DMS was subsequently analysed using established gas chromatography methods.

Table 1 DMSO concentration ranges in the marine environment

Location	DMSO concentration (nmol dm^{-3})	Reference
Coastal and open Pacific	19–181[a]	Andreae 1980a
Coastal and open Pacific	2.7–138	Hatton et al. 1998
Open Pacific	4–20	Kieber et al. 1996
Open Pacific	4	Bates et al. 1994
Coastal Pacific	6.3–124	Lee & de Mora 1996
Coastal Atlantic	4–6	Ridgeway et al. 1992
Coastal Atlantic	1.4–13	Kiene & Gerard 1994
North Atlantic	3.8–26	Simó et al. 2000
North Sea	2.3–25	Simó et al. 1998b, 2000
North Sea	<0.5–17.5	Hatton et al. 1996
Arabian Sea	<0.5–18	Hatton et al. 1996, 1999
Arctic fjord	<0.016	Lee et al. 1999a
Coastal Arctic	13.1–106	Bouillon et al. 2002
Coastal Arctic ice	2.0–116[b]	Lee et al. 2001
Coastal Antarctic	0.9–6	Gibson et al. 1990
Mediterranean Sea	2.2–62	Simó et al. 1995, 1997

[a]Not corrected for DMSP interference.
[b]Sample taken from sea ice.

Distribution of DMSO in sea water

A compilation of DMSO surface concentration data values from studies examining DMSO distribution in marine waters is presented in Table 1. Figure 1 shows concentration values superimposed onto a world map and indicates that the current data set is rather sparse compared with similar compilations of DMS data (Kettle et al. 1999). In surface waters the concentration of DMSO is generally equal to or slightly higher than that of DMS (Hatton et al. 1996, 1999). Figure 2 shows the concentrations of DMS and DMSO found in surface waters, from four data sets collected by the authors. Seawater samples were collected from a wide range of geographical locations (Arabian Sea, Antarctic, North Sea, and northeast Atlantic), including both coastal and open-ocean sites. From these results it is clear that the distribution of DMSO in surface waters closely follows that of DMS. The data show a positive correlation between DMS and DMSO ($r^2 = .8005$, $p < .001$) for the whole data set (Figure 3), suggesting that a similar relationship exists between the two compounds at different locations. However, it should also be noted that some studies have found DMSO levels that are one to two orders of magnitude greater than those of DMS (Andreae 1980a, Lee & de Mora 1996). In addition, studies during *Phaeocystis pouchetii* blooms in Antarctica (Gibson et al. 1990) and in the Saguenay Fjord, Québec (Lee et al. 1999a) found that DMSO levels were lower than those of related dimethylated sulphur compounds. In both cases, it was concluded that poor light penetration limited the photochemical oxidation of DMS and prevented the accumulation of DMSO.

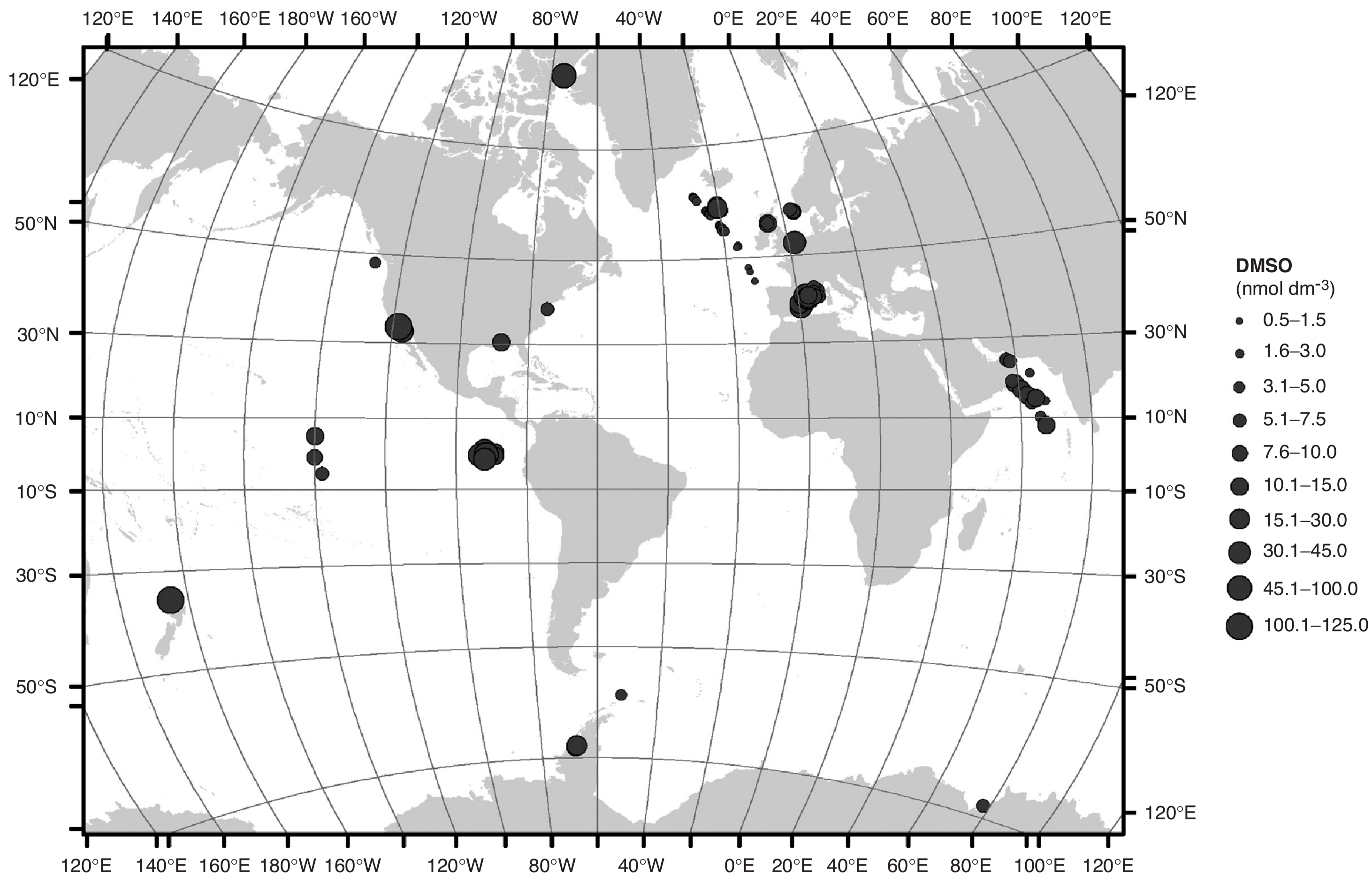

Figure 1 Location and levels of DMSO in surface waters collated from published data (see Table 1). Note: Where more than one concentration was detected at the same geographical location, highest values are plotted

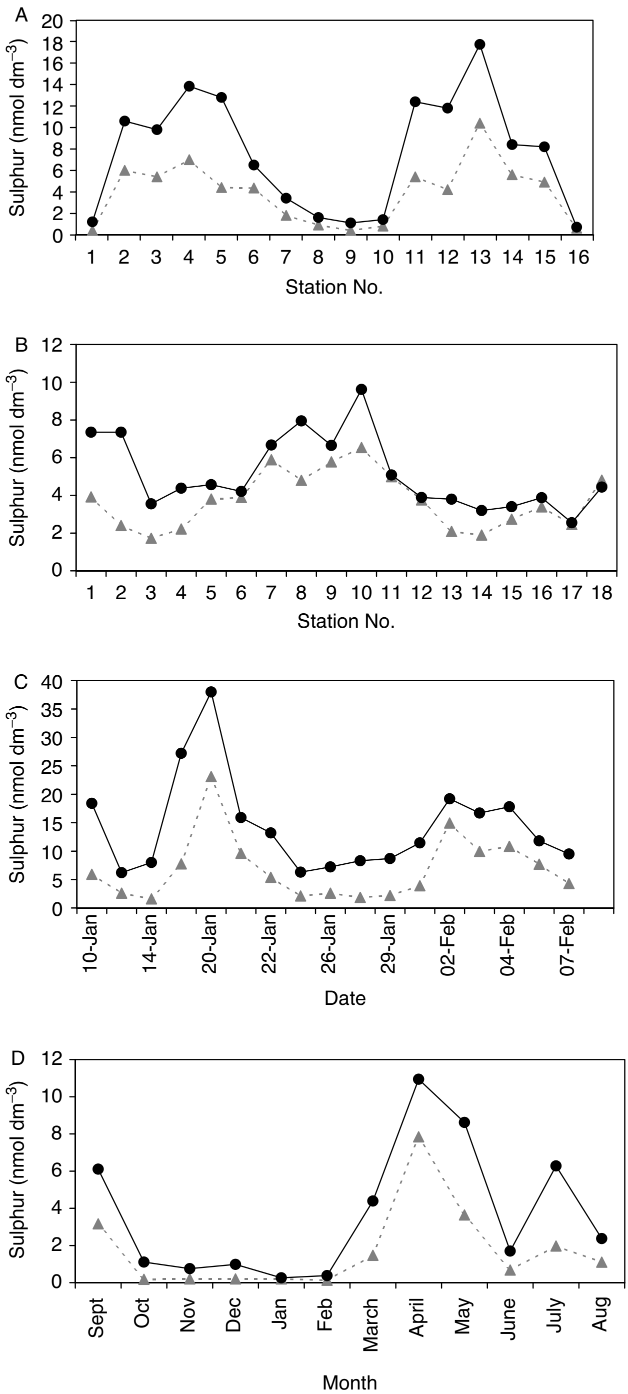

Figure 2 Near-surface concentrations for DMS (▲) and DMSO (●) collected during two oceanographic cruises to (A) the North Sea (from 52° 46N, 01° 50E to 54° 03N, 02° 10E to 52° 51N, 03° 07E, April 1994) and (B) the Arabian Sea (from 19° 30N, 58° 09E to 16° 02N, 62° 00E, August 20, and September 1994), and from two shore-based sites in (C) the Antarctic (at 67° 34S, 68° 15W, between January and February 1999) and (D) Scottish coastal waters (at 56° 31N, 05° 33W, between September 1998 and August 1999). (Sections A and B adapted from Hatton et al. 1996 and published with permission of Plenum Press.)